

## Supporting Information

### **Dual Functionalization of Mesoporous Organosilicon Nanoflowers Enhances Heterogeneous Chemoenzymatic Conversion of Alkynes toward Enantiopure Alcohols**

Chen Huang<sup>#1</sup>, Qian Zhang<sup>#1</sup>, Xiaoyang Yue<sup>\*1,2</sup>, Aidang Lu<sup>1,2</sup>, Guanhua Liu<sup>1,2</sup>, Ying He<sup>1,2</sup>, Li Ma<sup>1,2</sup>, Liya Zhou<sup>1,2</sup>, Yunting Liu<sup>\*1,2</sup>, Yanjun Jiang<sup>\*1,2</sup>

<sup>1</sup>School of Chemical Engineering and Technology, Hebei University of Technology, Tianjin, 300401, P. R. China.

<sup>2</sup>National-Local Joint Engineering Laboratory for Energy Conservation in Chemical Process Integration and Resources Utilization, Hebei University of Technology, Tianjin 300401, China

<sup>#</sup>These authors contributed equally to this work

Corresponding author e-mail addresses:

[xiaoyang.yue@hebut.edu.cn](mailto:xiaoyang.yue@hebut.edu.cn), [ytliu@hebut.edu.cn](mailto:ytliu@hebut.edu.cn), [yanjunjiang@hebut.edu.cn](mailto:yanjunjiang@hebut.edu.cn)

## 1. Chemicals and materials

Hexadecyl trimethylammonium bromide (CTAB), urea, glutaraldehyde (GA), tetrachloroauric acid ( $\text{HAuCl}_4$ ), *N*-trimethoxysilylpropyl-*N,N,N*-trimethylammonium chloride (TMAC) were purchased from Aldrich-sigma. Alcohol dehydrogenase (ADH) was purchased from Novozymes. 1,2-Bis(triethoxysilyl)ethane (BTSE), tetraethyl orthosilicate (TEOS), 3-mercaptopropyltriethoxysilane (MPTMS), *n*-butanol and cyclohexane were purchased from Tianjin Chemical Company. (3-aminopropyl) triethoxysilane (APTES) and phenylacetylene were purchased from Shanghai Maclean Biochemical Technology Company. All chemicals were used without further purification.

## 2. Characterization

Scanning electron microscopy (SEM) images were recorded on Nova Nano SEM 450 field-emission microscope at an accelerating voltage of 200 kV. All samples were dispersed in absolute ethyl alcohol ultrasonically and were dropped on a piece of monocrystalline silicon. Transmission electron microscopy (TEM) images were recorded on JEM-2100 microscope operated at an acceleration voltage of 1.0 kV. All sample powders were dispersed in ethyl alcohol ultrasonically and were dropped onto copper grid using a micropipette. The Au loading was determined by an Inductively Coupled Plasma Atomic Emission Spectrometry (ICP-AES). X-ray powder diffraction (XRD) data were acquired on a SCINTAG PADX diffractometer using Cu K $\alpha$  radiation. X-ray photoelectron spectroscopy (XPS) spectra were recorded on a Thermo Scientific K-Alpha X-ray photoelectron using a SQUID magnetic susceptometer. Nitrogen adsorption-desorption experiments were carried out on a micromeritics ASAP 2020 gas sorptometer. The specific surface area was calculated by Brunauer-Emmett-Teller (BET) method. The total pore volume of the samples was estimated by Barrett-Joyner-

Halenda (BJH) model. Confocal laser scanning microscopy (CLSM) micrographs were recorded on a Leica TCS SP5 optical microscope with excitation wavelength of 488nm and emission wavelength of 525nm. Before tested, ADH were marked with fluorescein isothiocyanate (FITC) and then immobilized on the nanoflowers. Fourier transform infrared (FT-IR) spectra were measured with a Bruker TENSOR27 spectrometer.

### **3. Preparation of dendritic organosilicon nanoflowers (DONs)**

CTAB (1.25 g), n-butanol (1.25 g) and cyclohexane (5.00 g) were dissolved in an aqueous solution of urea (0.4 M, 100.0 g) at room temperature. After a sonication for 10 min, TEOS (0.875 g) and BTSE (0.375 g) were added into the mixture. The mixture was kept stirring at room temperature for 30 min and then at 70 °C for 24 h. After cooled to room temperature, the obtained powder was washed with ethanol and deionized water, immersed in an ethanol solution of ammonium nitrate at 70 °C for 48 h and then centrifuged. Washed with ethanol for three times and dried at room temperature to obtain the dendritic organosilicon nanoflowers (DONs).

### **4. Preparation of HS-DON and Au@HS/SO<sub>3</sub>-DON**

HS-DON was synthesized via a similar procedure as DONs, and MPTMS (0.13 g) was added as the sulfhydryl sources. The obtained HS-DON (25 mg) was then dispersed in anhydrous ethanol (2 mL), and the solution of HAuCl<sub>4</sub> (1 mL, 13 mM in ethanol) was then added dropwise to obtain Au@HS/SO<sub>3</sub>H-DON. After stirring at room temperature for 48 h. The obtained powder was separated by centrifugation, washed with anhydrous ethanol for several times, and dried under vacuum at 60 °C overnight.

### **5. Preparation of NH<sub>2</sub>-DON**

The prepared DON (0.29 g) was dispersed in 100 mL of hexane in a 250 mL round-bottom flask, and treated with ultrasonic for 30 min. 1 mL of APTES was added into the DON suspension and kept refluxing at 80 °C for 12 h. The product was centrifugated

and washed with anhydrous ethanol for several times, and dried at room temperature to obtain the NH<sub>2</sub>-DON.

## **6. Preparation of ADH@QA-DON**

The prepared NH<sub>2</sub>-DON (0.5 g) was dispersed in 100 mL of hexane in a 250 mL round-bottom flask, and treated with ultrasonic for 30 min. 1 mL methanol solution of quaternary ammonium salt (CAS: 35141-36-7) was added into the NH<sub>2</sub>-DON suspension and kept refluxing at 80 °C for 24 h to obtain the QA-DON. The obtained activated QA-DON were separated by centrifugation, washed with ethanol and deionized H<sub>2</sub>O for several times and dried at room temperature. The activated QA-DON (10 mg) was then dispersed in PBS (50 mM, pH 8) and incubated in ADH solution (3 mL) under shaking. The obtained ADH@QA-DON was centrifuged, washed with PBS three times and lyophilized.

## **7. Activity assay of ADH**

NADH (1 mM), acetophenone (10 mM) and immobilized enzyme (10 mg) were added to 1 mL PBS (50 mM, pH=8.0), and the reaction was conducted at 40 °C for 1 min. The supernatant was obtained by filtration, and whose OD value was measured at 340 nm using a UV-vis spectrophotometer. Herein, ADH activity was defined as the amount of enzyme that was required to produce 1 μmol 1-phenylethanol per minute under the assay conditions, which is referred as 1 U.

## **8. The procedure for the hydration of phenylacetylene over Au@HS/SO<sub>3</sub>H-DON**

Phenylacetylene (50 mM) was dispersed in the mixture of deionized water (1.4 mL) and *i*-PrOH (0.6 mL), then the catalyst Au@HS/SO<sub>3</sub>H-DON (0.8 mol%) was added and the reaction was stirred at 80 °C for 3 h. The reaction process was monitored by thin plate chromatography (TLC). After the reaction was completed, the Au@HS/SO<sub>3</sub>H-DON catalyst was separated by centrifugation.

## **9. The procedure for the reduction of acetophenone over ADH@QA-DON**

After removing Au@HS/SO<sub>3</sub>H-DON, 10 mg of ADH@QA-DON and 2 mL mixture of PBS (pH 8.0, 50 mM) and NADH (0.5 mM) were added. The mixture was then stirred at 40 °C for 5 h. The reaction process was monitored by (TLC), and the yields and ee values of the obtained chiral alcohols were determined by HPLC and GC.

## **10. The reusability test of Au@HS/SO<sub>3</sub>H-DON and ADH@QA-DON**

In each reaction cycle, the used Au@HS/SO<sub>3</sub>H-DON and ADH@DON were isolated by centrifugation. The Au@HS/SO<sub>3</sub>H-DON was washed using methanol and the ADH@QA-DON was washed using PBS to remove the residual substrate and product, respectively. The obtained catalysts were then utilized in the next reaction cycle, separately.

## **11. Adsorption Experiments**

A series of batch experiments were carried out to study the adsorption behaviors of NADH molecules in solutions with the DON, QA-DON and QA-SNA-15, separately. Typically, a certain amount of adsorbent material (200 mg) and the NADH solution (25 mL, 2 mg.L<sup>-1</sup>) were mixed in centrifuge tube (50 mL), which was stirred continuously at 30 °C with a thermostatic shaker for a certain time. At predetermined time intervals, the mixture was withdrawn and centrifuged to separate the supernatant. The concentration of the residual NADH solution was analyzed by UV–Visible spectrophotometer. Absorbance at the maximum absorption wavelength of  $\lambda_{\text{max}} = 340$  nm was measured. This process was repeated until adsorption equilibrium was reached. The concentrations of each sample were determined before and after adsorption from the standard calibration curve.

## **12. Adsorption Kinetics**

Adsorption kinetics could reveal the rate of an adsorption process and provide

important engineering parameters for the practical applications of the adsorbents. To evaluate the adsorption kinetics, pseudo-first-order, pseudo-second-order and intraparticle diffusion models were adopted. For the pseudo-first-order kinetic model, it assumed that the rate of solute change uptake with time is proportional to the saturation concentration difference, which is generally used to verify the adsorption of an adsorbate from an aqueous solution based upon the assumption of a physisorption process. The linear form of the pseudo-first-order equation can be expressed as follows:

$$\ln(1 - Q_t/Q_e) = Rt \quad (eq.s1)$$

where  $Q_e$  and  $Q_t$  ( $\text{mg g}^{-1}$ ) are the amounts of the organic dyemolecules being adsorbed on the adsorbent at equilibrium and  $t$  (min), respectively;  $R$  ( $\text{g}/(\text{mg}\cdot\text{min}^{-1})$ ) is the the liquid film diffusion coefficient. The pseudo-second-order model described the adsorption process that derived from a chemical reaction between the adsorbent and adsorbate, indicating that the adsorption process occurred through a chemisorption mechanism. The linear form of pseudo-second-order equation is expressed as follows:

$$\frac{t}{Q_t} = \frac{1}{K_1 Q_e^2} + \frac{t}{Q_e} \quad (eq.s2)$$

where  $k_1$  ( $\text{g mg}^{-1} \text{min}^{-1}$ ) is the rate constant of the pseudo-second-order model.

The intraparticle diffusion model is employed to describe the kinetics of adsorbate diffusion within the pores of the adsorbent particles. This model assumes that the rate-limiting step in the adsorption process is the diffusion of the adsorbate through the pores of the adsorbent. The mathematical expression for this model is given by the following equation:

$$Q_t = k_2 t^{0.5} + C \quad (eq.s3)$$

where  $k_2$  ( $\text{mg g}^{-1} \text{min}^{-0.5}$ ) is the intraparticle diffusion rate constant and  $C$  relates to the thickness of the boundary layer.

### 13. Continuous-flow chemoenzymatic synthesis of (S)-1-phenylethanol in PBRs

Solution 1: phenylacetylene (50 mM) in mixed solution of 30% (v/v) *i*-PrOH and 70% (v/v) water, pumped through P1 (0.03 or 0.06 mL/min). Solution 2: NADH (1 mM) in PBS (100 mM, pH 8.2), pumped through P2 (0.03 or 0.06 mL/min). The Au@HS/SO<sub>3</sub>H-DON (1.024 g) was packed into the PBR1 (4.6 × 100 mm, Zhijia, Hangzhou, China) and the column temperature was maintained at 80 °C under oil bath. The ADH@QA-DON (1 g) was packed into the PBR2 (4.6 × 100 mm) and the column temperature was maintained at 30 °C under water bath. The solution one passed into the pipeline (1/16 outer diameter, 0.75 mm inner diameter) and then entered the PBR1. P2 was loaded downstream of the PBR1 to feed PBS solution to mix with the outlet stream of the PBR1 for adjusting the pH value to 8.0. The mixed solution then flowed into the PBR2 and the effluent was processed for testing. The space time yield (STY) in continuous flow reactions was calculated as follows:

$$STY(g / L / h) = \frac{\text{substrate concentration}(M) \times \text{yield}(\%) \times \text{flow rate}(L / h) \times MW(g / mol)}{\text{reactor volume}(L) \times 100}$$

The space time yield (STY) in batch reaction reactions was calculated as follows:

$$STY(g / L / h) = \frac{\text{substrate concentration}(M) \times \text{yield}(\%) \times MW(g / mol)}{\text{time}(h) \times 100}$$

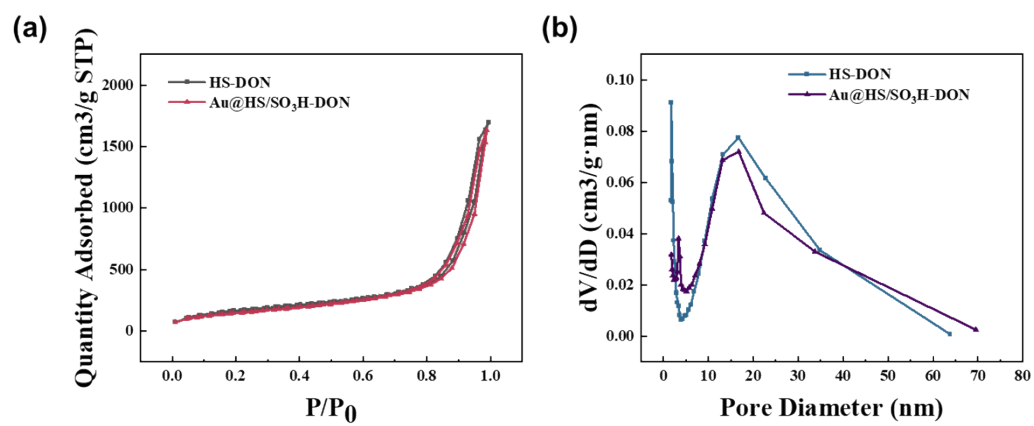


**Figure S1.** (a) The nitrogen absorption-desorption isotherms of HS-DON and Au@HS/SO<sub>3</sub>H-DON;

(b) The pore size distribution of HS-DON and Au@HS/SO<sub>3</sub>H-DON.

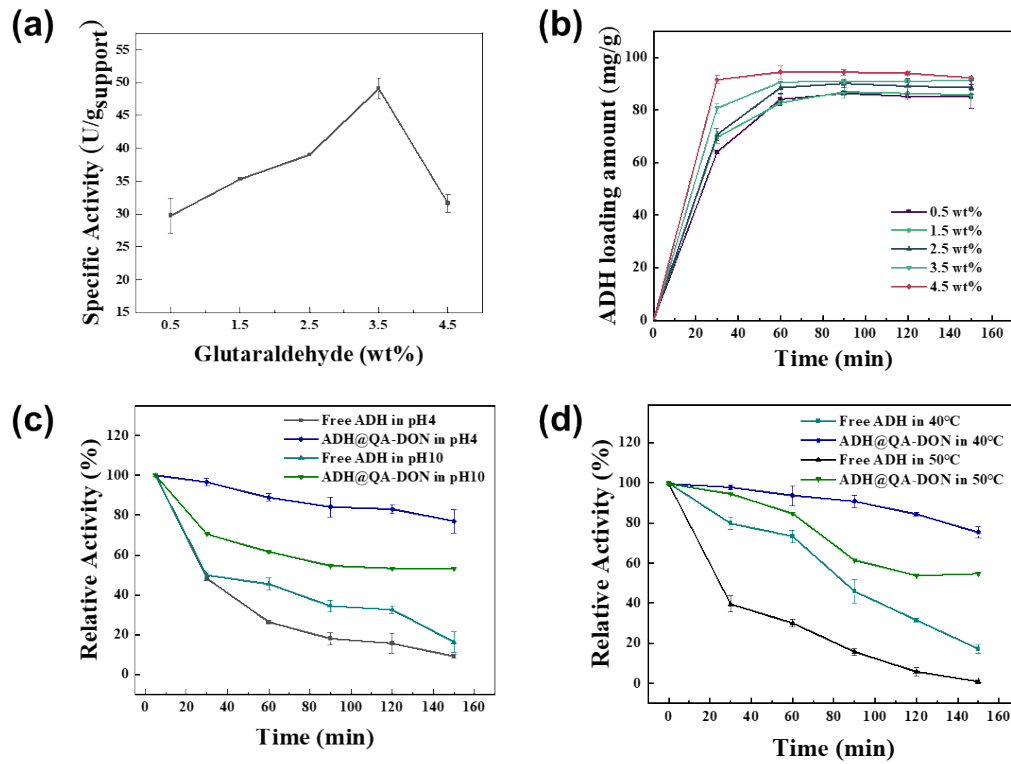


**Figure S2.** The influence of glutaraldehyde concentration on (a) the specific activity and (b) loading amount of immobilized ADH; (c) pH stability of ADH@QA-DON; (d) thermal stability of ADH@QA-DON.

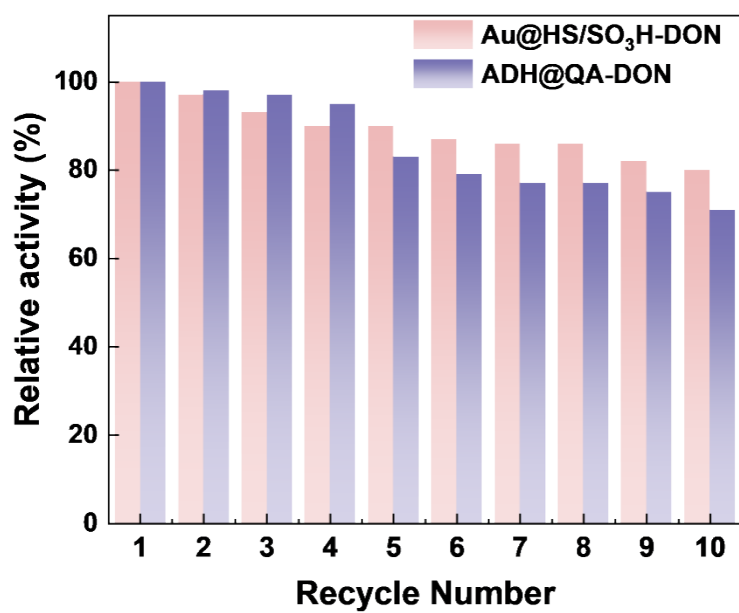


**Figure S3.** Reusability test for the Au@HS/SO<sub>3</sub>H-DON and ADH@QA-DON

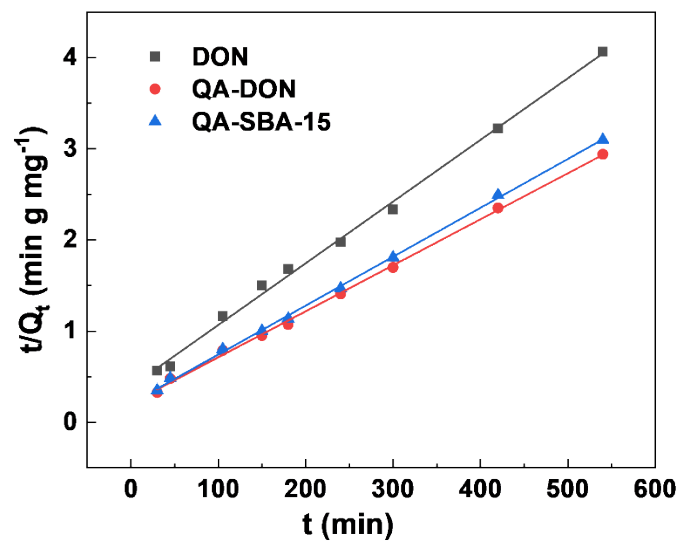


**Figure S4.** Kinetics analysis of NADH adsorption on various carriers at 30°C (pseudo-second-order model), conditions: adsorbent (200 mg),  $C_0$  (NADH) = 2 mg L<sup>-1</sup>, 25 mL

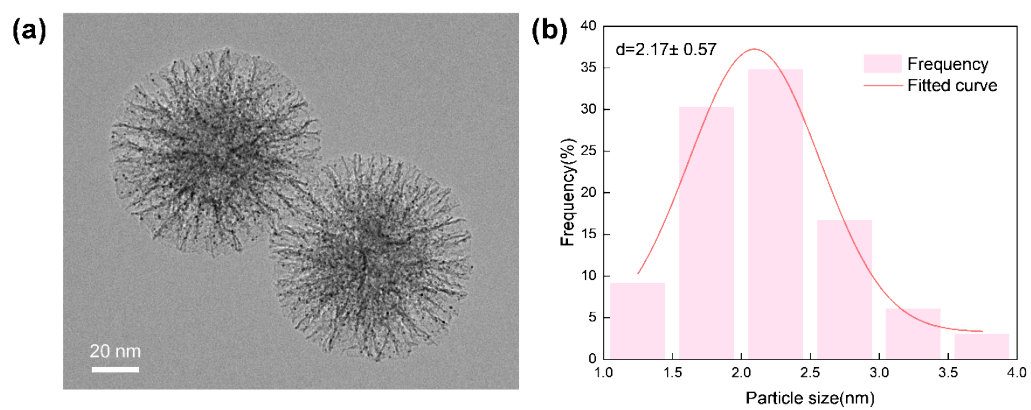


**Figure S5.** TEM image and Au particles size distribution of the reused Au@HS/SO<sub>3</sub>H-DON

**Table S1.** ICP and BET analysis of HS-DON and Au@HS/SO<sub>3</sub>H-DON

<b>Sample</b>	<b>Au loading</b>	<b>S<sub>BET</sub> (m<sup>2</sup>/g)</b>	<b>D<sub>P</sub> (nm)<sup>a</sup></b>	<b>V<sub>P</sub> (cm<sup>3</sup>/g)<sup>b</sup></b>
HS-DON (0.3)	0	608	14.7	1.87
Au@HS/SO <sub>3</sub> H-DON (0.3)	0.8 wt%	554	13.5	1.81
Au@HS/SO <sub>3</sub> H-DON (0.6)	1.9 wt%	533	11.1	1.65
Au@HS/SO <sub>3</sub> H-DON (0.9)	2.5 wt%	494	10.8	1.49

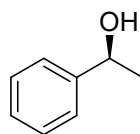
<sup>a</sup> Average pore diameter. <sup>b</sup> Pore volume.

**Table S2.** Pseudo-second order kinetics analysis of NADH adsorption on various carriers at 30°C

<b>Adsorbent</b>	$Q_e (exp.) \text{ mg g}^{-1}$	$Q_e (cal.) \text{ mg g}^{-1}$	$K_1 \text{ g (mg min)}^{-1}$
DON	132.78	147.71	0.000117
QA-DON	183.68	198.02	0.000123
QA-SBA-15	174.18	186.57	0.000139

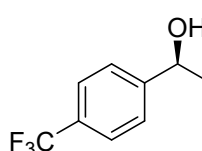
Conditions: adsorbent (200 mg),  $C_0$  (NADH) = 2 mg L<sup>-1</sup>, 25 mL

$^1\text{H}$  NMR spectra of the products recorded in  $\text{CDCl}_3/\text{D}_2\text{O}$



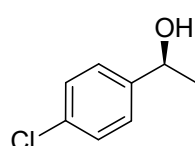
**3a**,  $^1\text{H}$  NMR (400 MHz, Chloroform- $d$ )  $\delta$  7.42 - 7.28 (m, 5H), 4.89 (q,  $J$  = 6.5 Hz, 1H), 2.30 (s, 1H), 1.51 (d,  $J$  = 6.5 Hz, 3H).

$^{13}\text{C}$  NMR (101 MHz,  $\text{CDCl}_3$ )  $\delta$  145.93, 128.50, 127.43, 125.48, 70.31, 25.16.



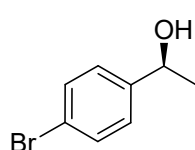
**3b**,  $^1\text{H}$  NMR (400 MHz, Chloroform- $d$ )  $\delta$  7.61 (d,  $J$  = 8.2 Hz, 2H), 7.48 (d,  $J$  = 8.2 Hz, 2H), 4.95 (q,  $J$  = 6.5 Hz, 1H), 2.31 (s, 1H), 1.50 (d,  $J$  = 6.5 Hz, 3H).

$^{13}\text{C}$  NMR (101 MHz,  $\text{CDCl}_3$ )  $\delta$  149.71, 129.80, 129.48, 125.66, 125.46, 125.42, 122.84, 120.14, 69.81, 25.33.



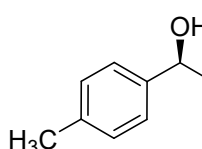
**3c**,  $^1\text{H}$  NMR (400 MHz, Chloroform- $d$ )  $\delta$  7.31 (d,  $J$  = 8.7 Hz, 2H), 7.27 (d,  $J$  = 8.6 Hz, 2H), 4.83 (q,  $J$  = 6.5 Hz, 1H), 2.53 (s, 1H), 1.45 (d,  $J$  = 6.5 Hz, 3H).

$^{13}\text{C}$  NMR (101 MHz,  $\text{CDCl}_3$ )  $\delta$  144.28, 133.10, 128.62, 126.82, 69.76, 25.28.



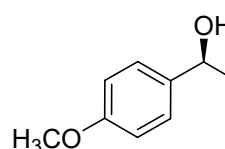
**3d**,  $^1\text{H}$  NMR (400 MHz, Chloroform- $d$ )  $\delta$  7.46 (d,  $J$  = 8.4 Hz, 2H), 7.22 (d,  $J$  = 8.4 Hz, 2H), 4.81 (q,  $J$  = 6.5 Hz, 1H), 2.53 (s, 1H), 1.44 (d,  $J$  = 6.5 Hz, 3H).

$^{13}\text{C}$  NMR (101 MHz,  $\text{CDCl}_3$ )  $\delta$  144.80, 131.58, 127.18, 121.18, 69.80, 25.26.



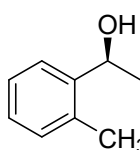
**3e**,  $^1\text{H}$  NMR (400 MHz, Chloroform- $d$ )  $\delta$  7.29 (d,  $J$  = 8.0 Hz, 2H), 7.20 (d,  $J$  = 8.0 Hz, 2H), 4.86 (q,  $J$  = 6.5 Hz, 1H), 2.40 (s, 4H), 1.51 (d,  $J$  = 6.5 Hz, 3H).

$^{13}\text{C}$  NMR (101 MHz,  $\text{CDCl}_3$ )  $\delta$  142.95, 137.11, 129.18, 125.41, 70.23, 25.09, 21.12.



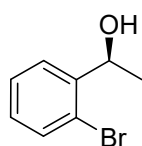
**3f**,  $^1\text{H}$  NMR (400 MHz, Chloroform- $d$ )  $\delta$  7.30 (d,  $J$  = 8.7 Hz, 2H), 6.89 (d,  $J$  = 8.7 Hz, 2H), 4.84 (q,  $J$  = 6.4 Hz, 1H), 3.81 (s, 3H), 2.29 (s, 1H), 1.48 (d,  $J$  = 6.5 Hz, 3H).

$^{13}\text{C}$  NMR (101 MHz,  $\text{CDCl}_3$ )  $\delta$  159.01, 138.08, 126.69, 113.88, 69.97, 55.32, 25.04.



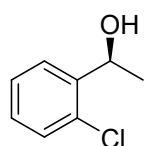
**3g**,  $^1\text{H}$  NMR (400 MHz, Chloroform- $d$ )  $\delta$  7.54 (d,  $J$  = 7.6 Hz, 1H), 7.27 (t,  $J$  = 7.4 Hz, 1H), 7.24 - 7.15 (m, 2H), 5.13 (q,  $J$  = 6.4 Hz, 1H), 2.37 (s, 3H), 2.15 (s, 1H), 1.49 (d,  $J$  = 6.4 Hz, 3H).

$^{13}\text{C}$  NMR (101 MHz,  $\text{CDCl}_3$ )  $\delta$  143.92, 134.25, 130.39, 127.18, 126.40, 124.55, 66.80, 23.95, 18.93.



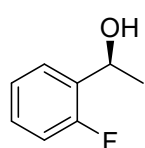
**3h**,  $^1\text{H NMR}$  (400 MHz, Chloroform- $d$ )  $\delta$  7.61 (d,  $J = 9.3$  Hz, 1H), 7.53 (d,  $J = 8.0$  Hz, 1H), 7.36 (t,  $J = 7.3$  Hz, 1H), 7.17 – 7.12 (m, 1H), 5.26 (q,  $J = 6.4$  Hz, 1H), 2.18 (s, 1H), 1.50 (d,  $J = 6.4$  Hz, 3H).

$^{13}\text{C NMR}$  (101 MHz,  $\text{CDCl}_3$ )  $\delta$  144.70, 132.67, 128.76, 127.88, 126.73, 121.71, 69.17, 23.62.



**3i**,  $^1\text{H NMR}$  (400 MHz, Chloroform- $d$ )  $\delta$  7.59 (d,  $J = 7.7$  Hz, 1H), 7.34 (d,  $J = 8.0$  Hz, 1H), 7.30 (d,  $J = 8.5$  Hz, 1H), 7.21 (t,  $J = 7.6$  Hz, 1H), 5.29 (q,  $J = 6.6$  Hz, 1H), 2.36 (s, 1H), 1.49 (d,  $J = 6.4$  Hz, 3H).

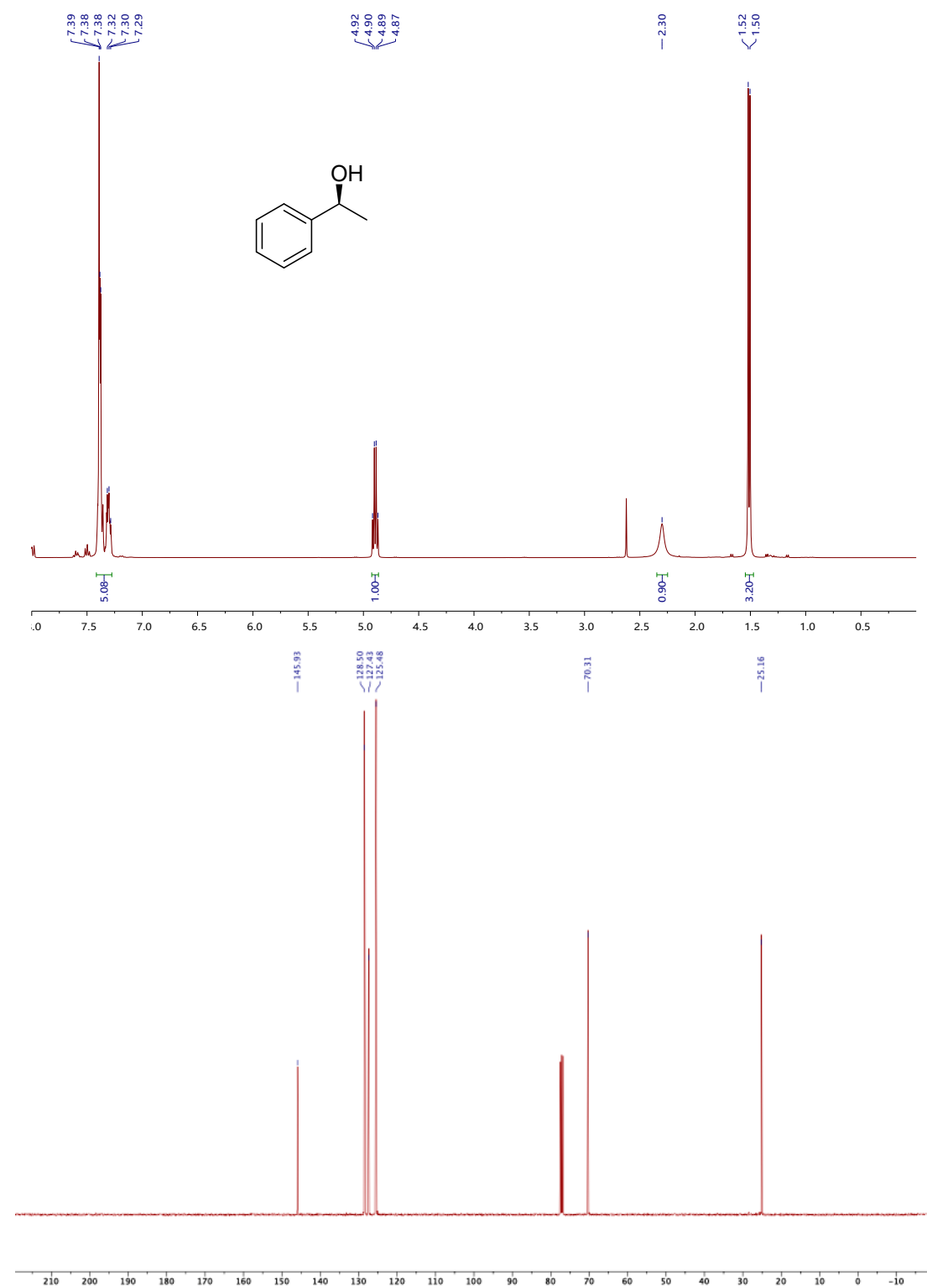
$^{13}\text{C NMR}$  (101 MHz,  $\text{CDCl}_3$ )  $\delta$  143.15, 131.61, 129.39, 128.37, 127.22, 126.47, 66.91, 23.54.

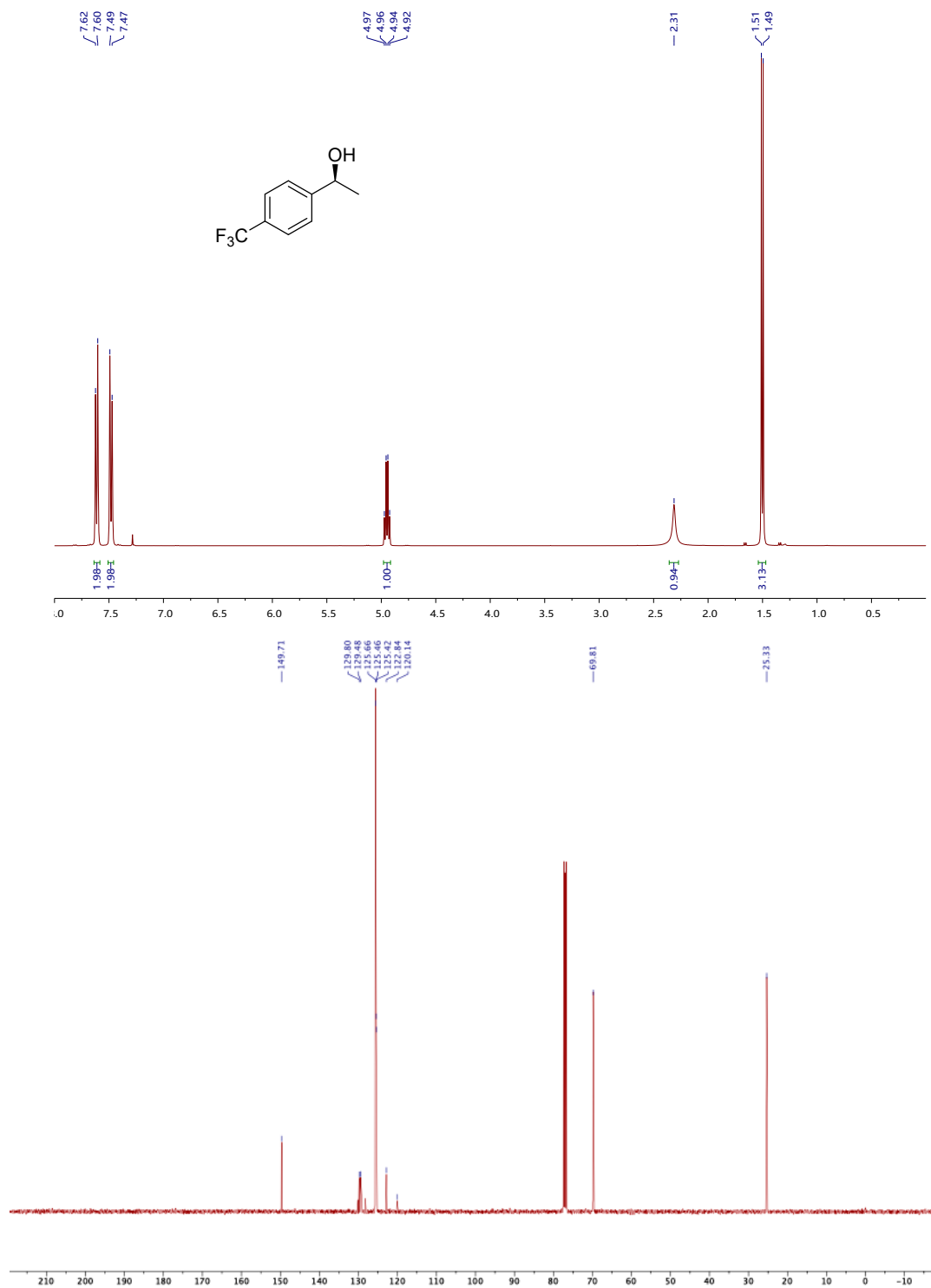


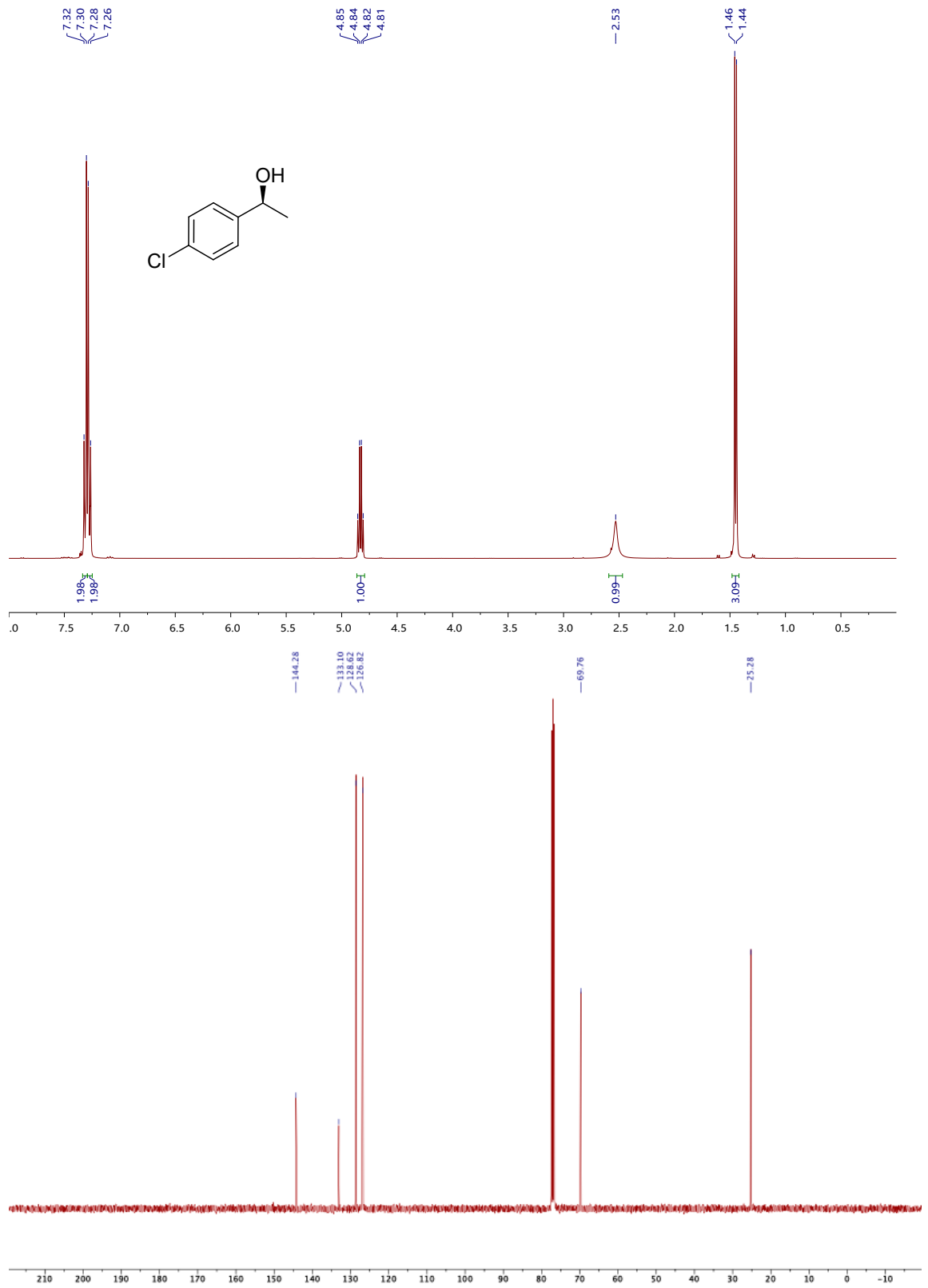
**3j**,  $^1\text{H NMR}$  (400 MHz, Chloroform- $d$ )  $\delta$  7.49 (t,  $J = 8.2$  Hz, 1H), 7.29 – 7.22 (m, 1H), 7.16 (t,  $J = 7.5$  Hz, 1H), 7.08 – 6.99 (m, 1H), 5.24 – 5.15 (m, 1H), 2.45 (d,  $J = 4.0$  Hz, 1H), 1.52 (d,  $J = 6.5$  Hz, 3H).

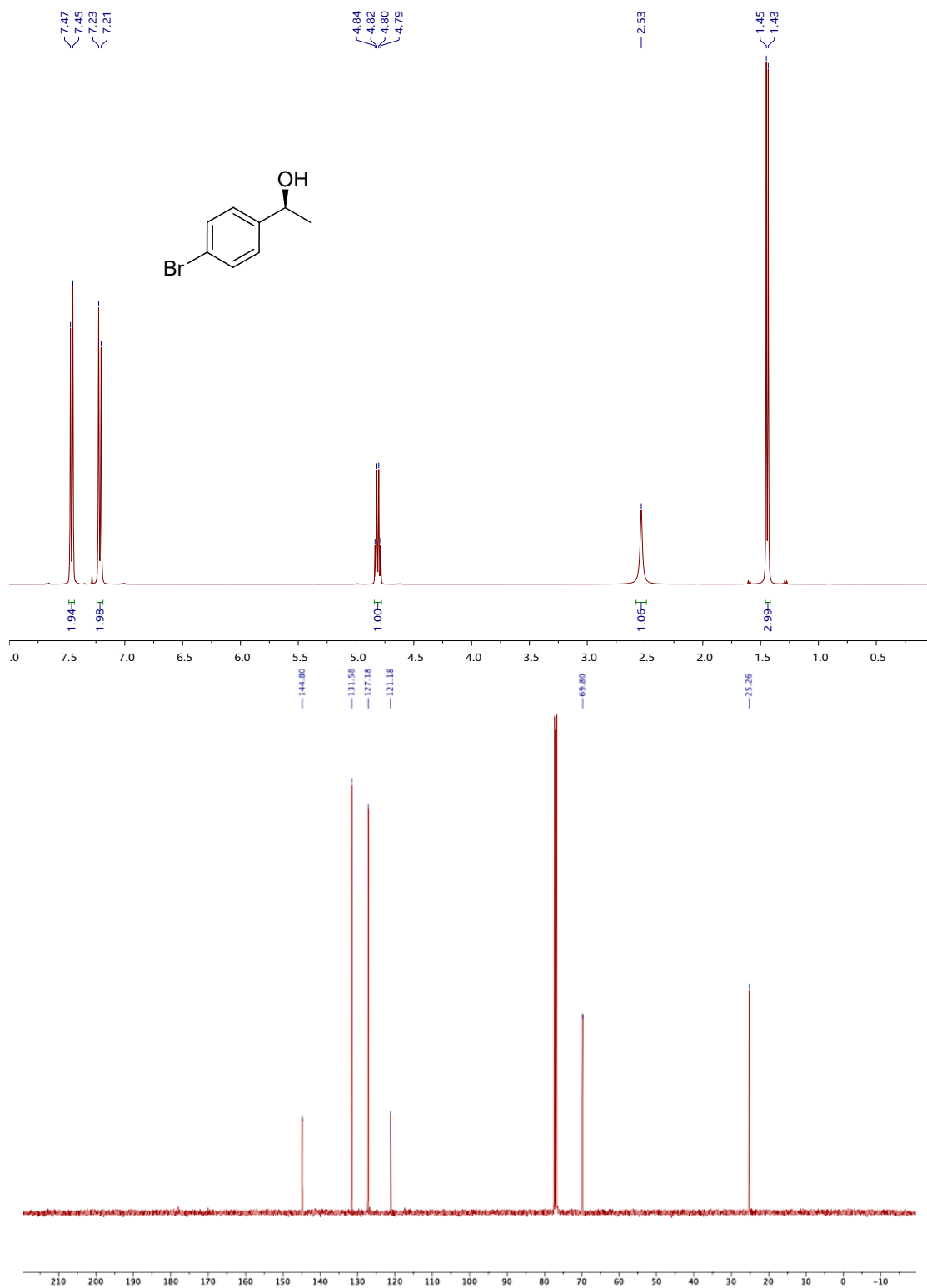
$^{13}\text{C NMR}$  (101 MHz,  $\text{CDCl}_3$ )  $\delta$  160.92, 158.48, 128.74, 126.66, 124.27, 115.12, 64.34, 23.98.

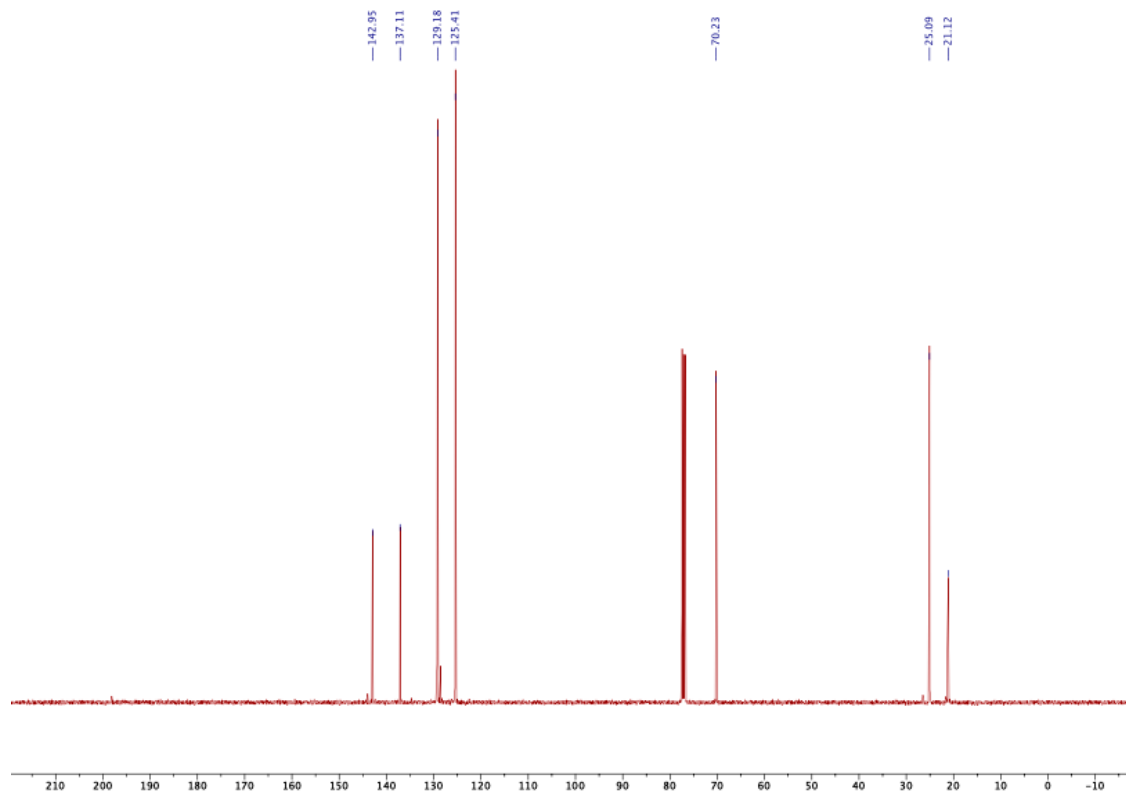
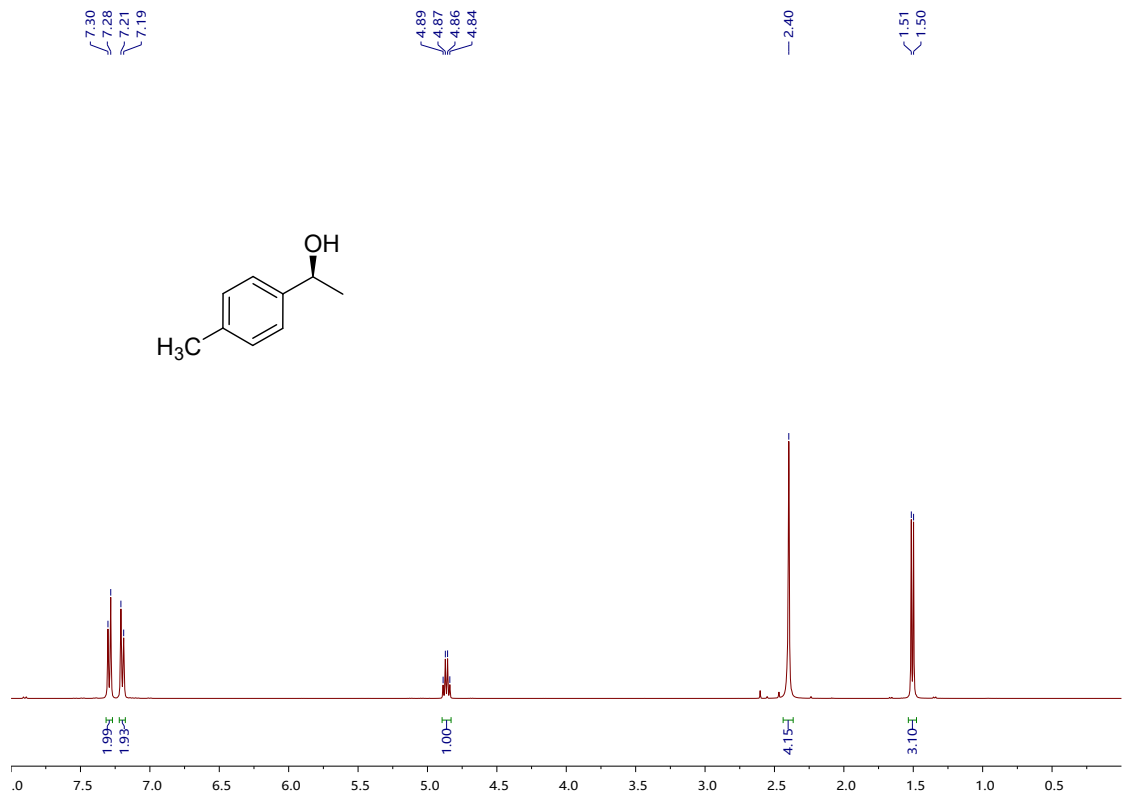
**<sup>1</sup>H-NMR spectra of products:**

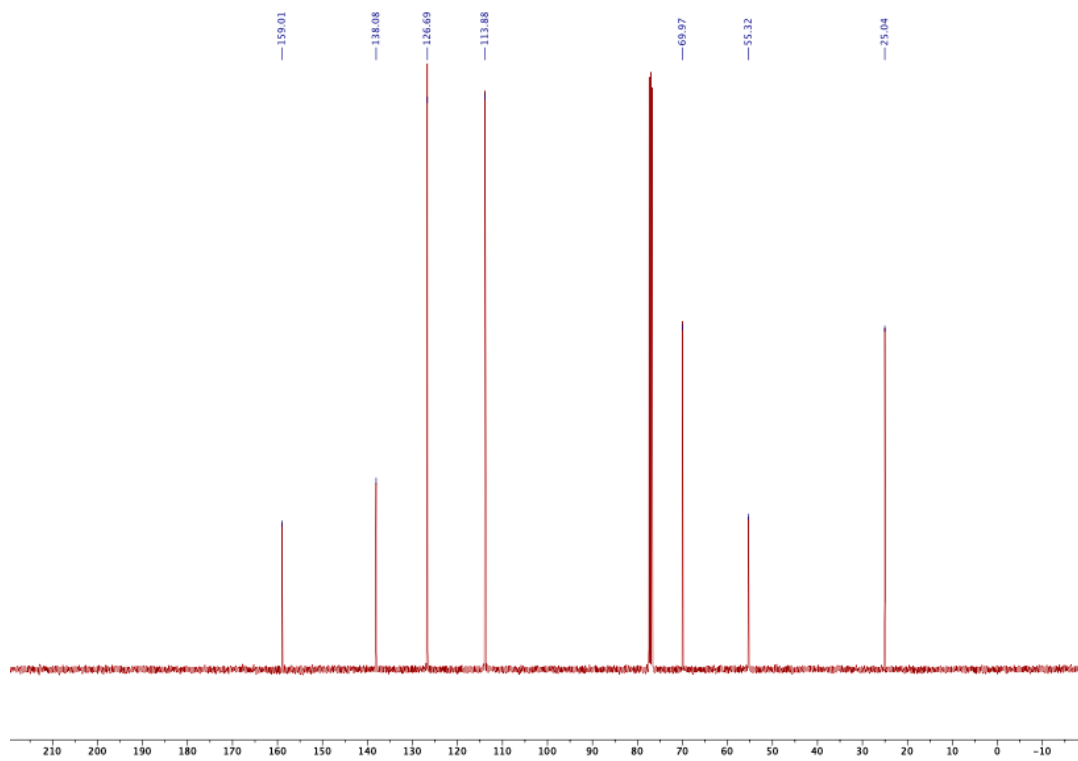
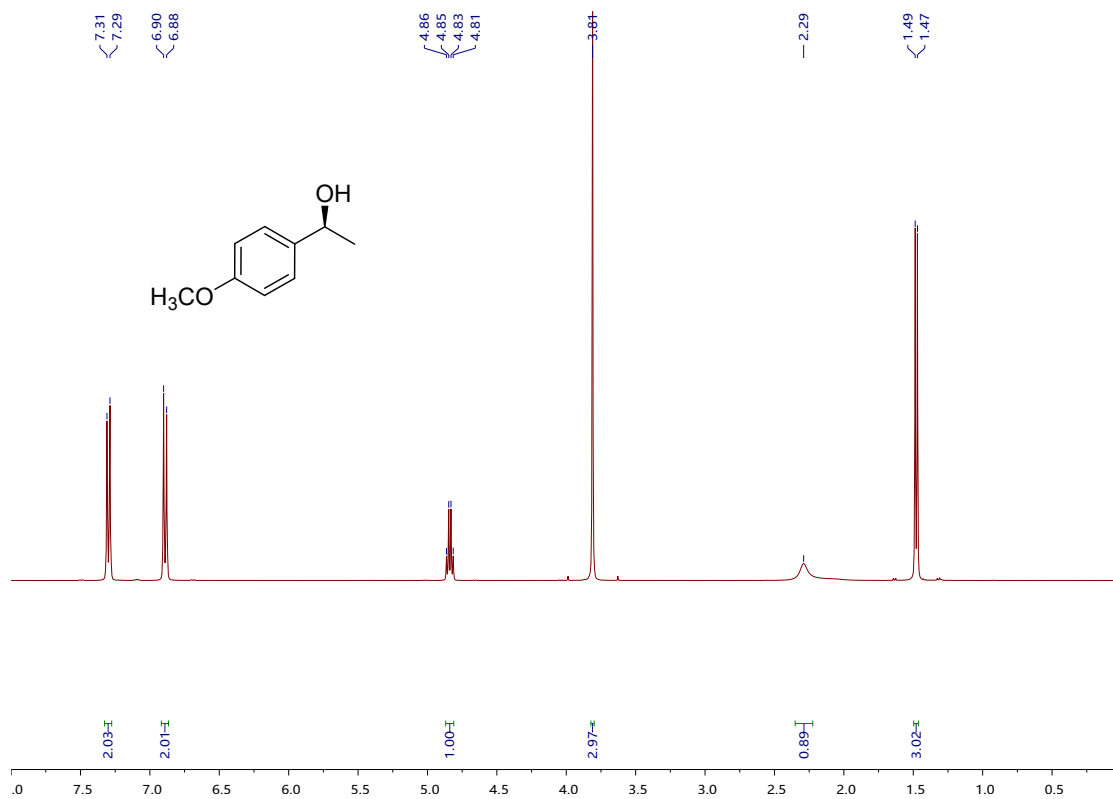


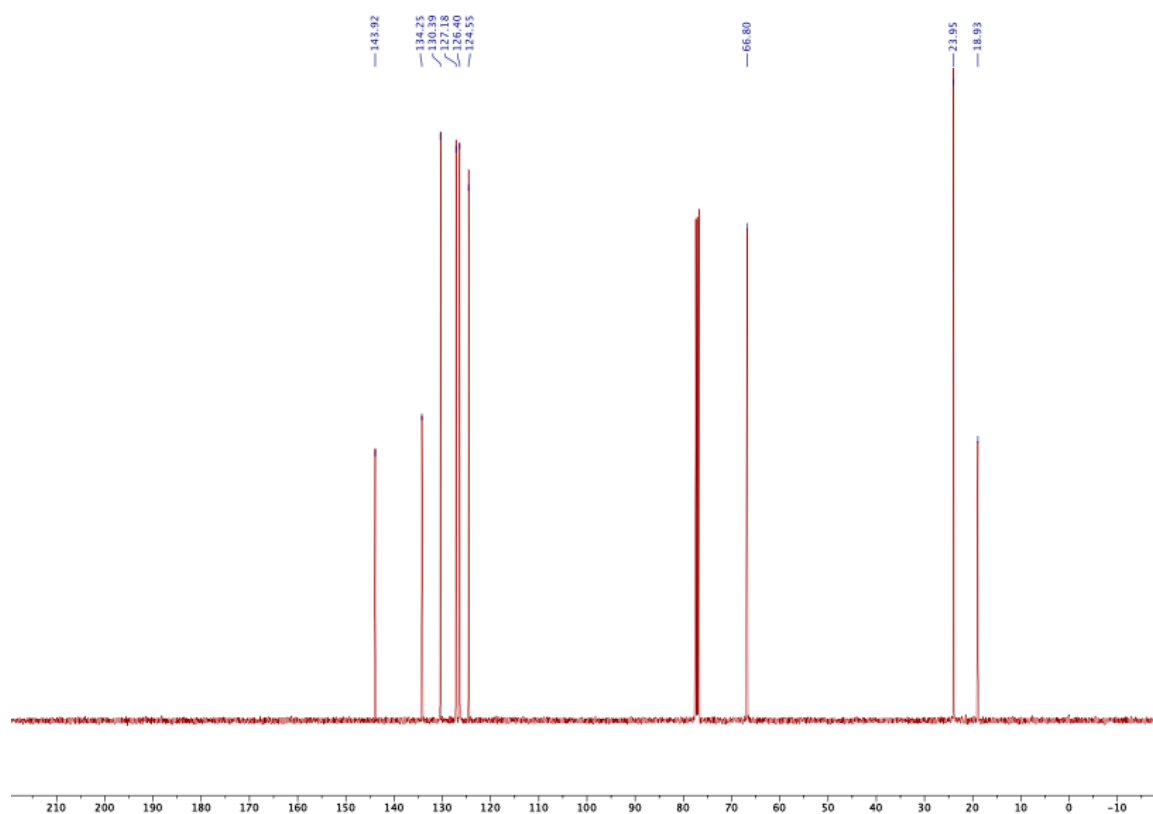
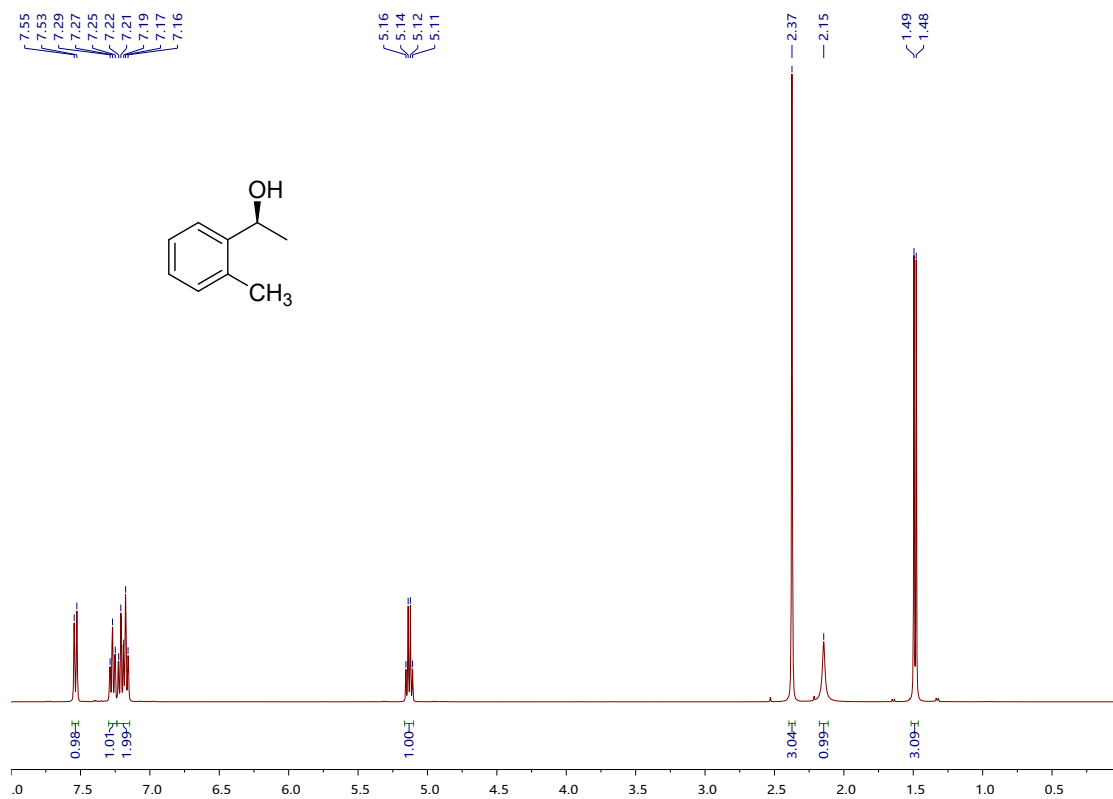


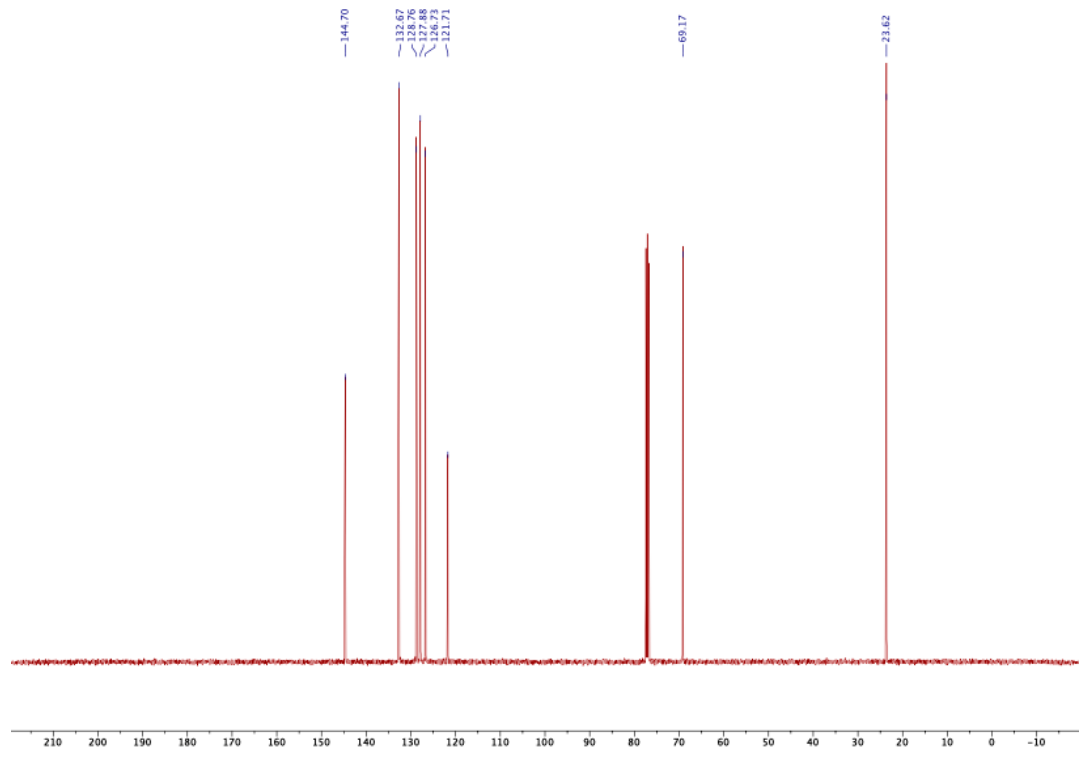
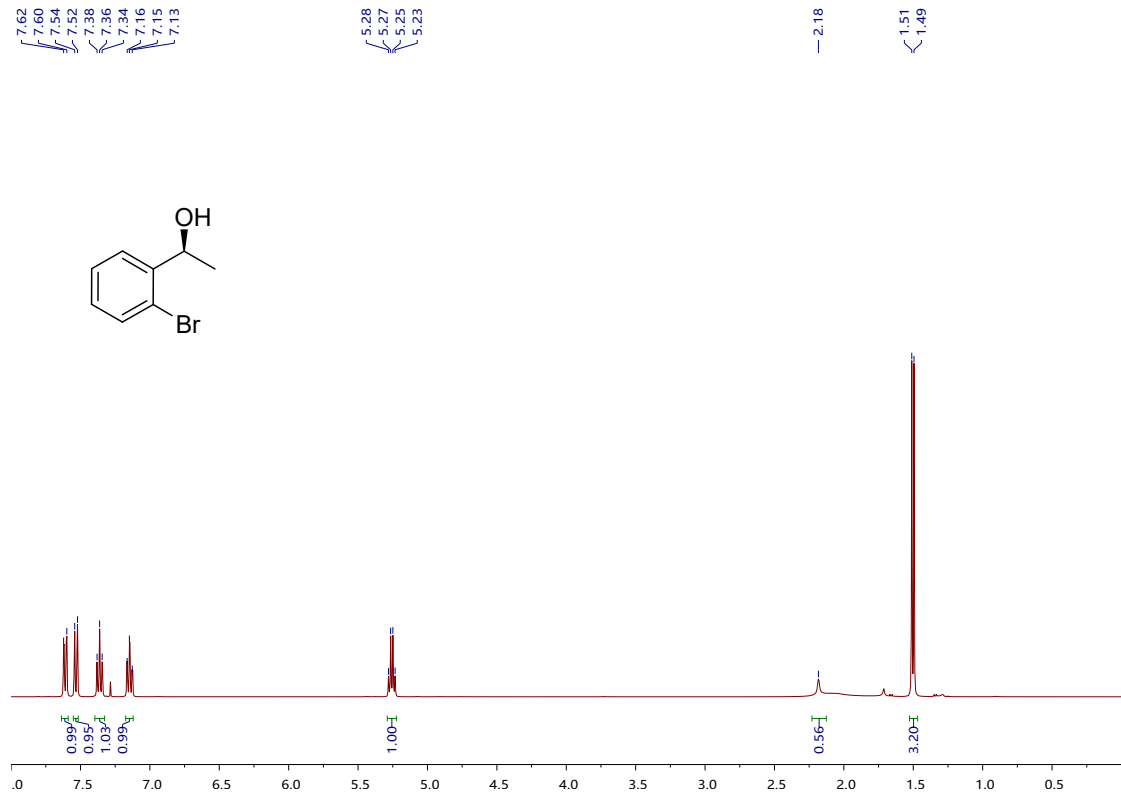


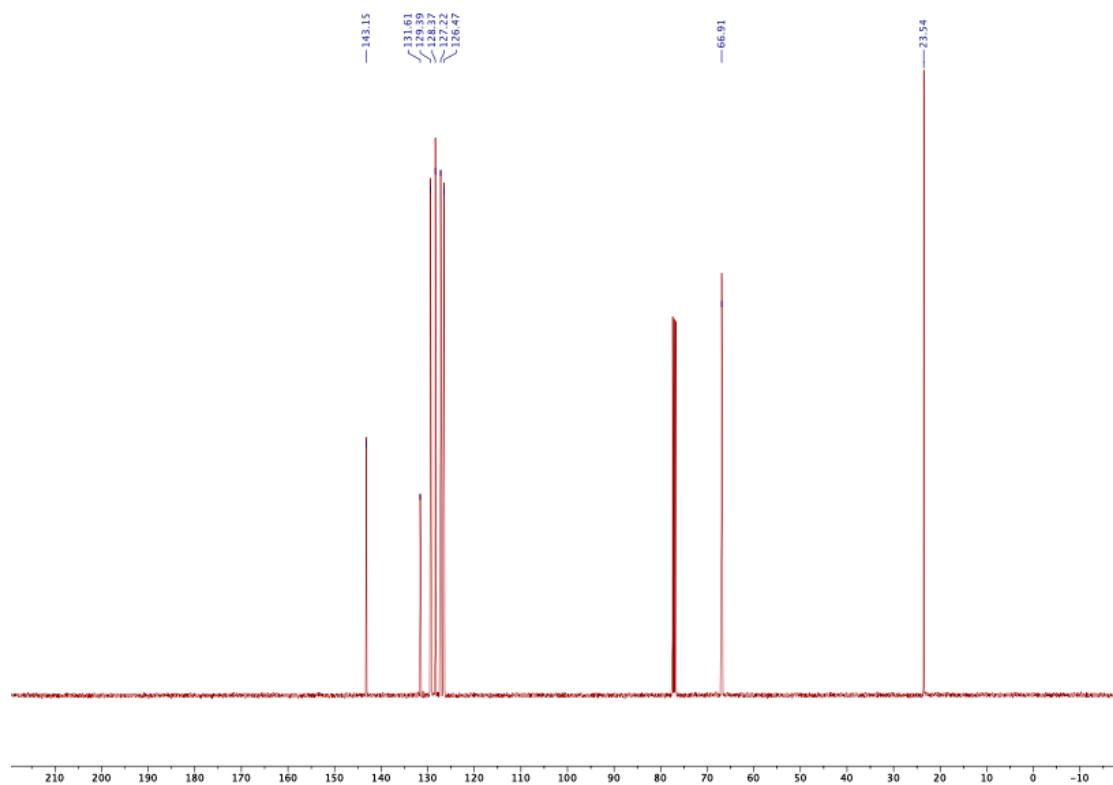
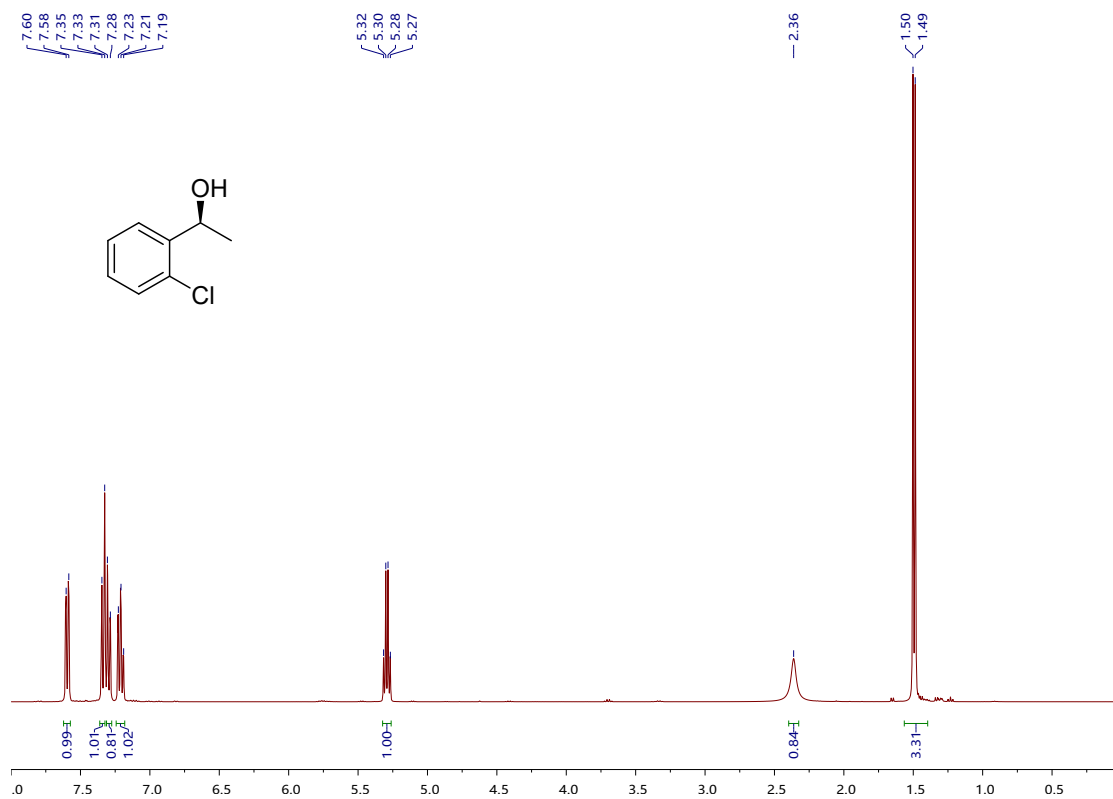


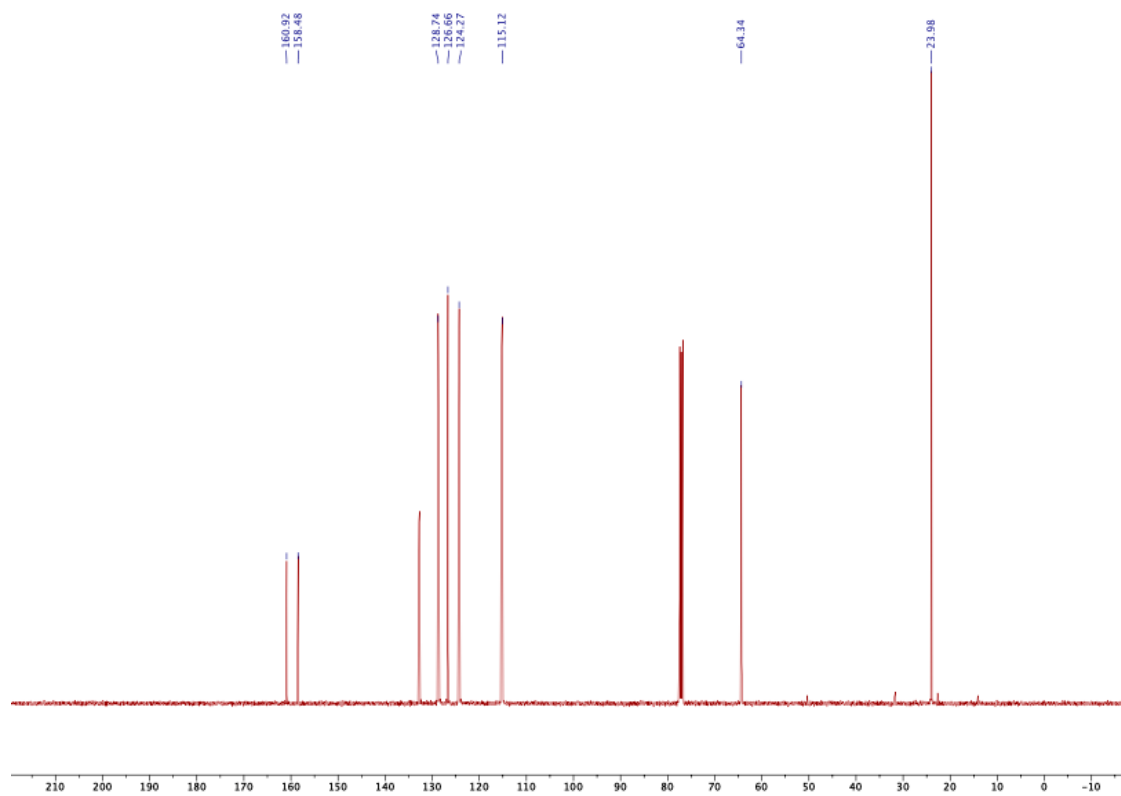
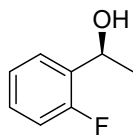
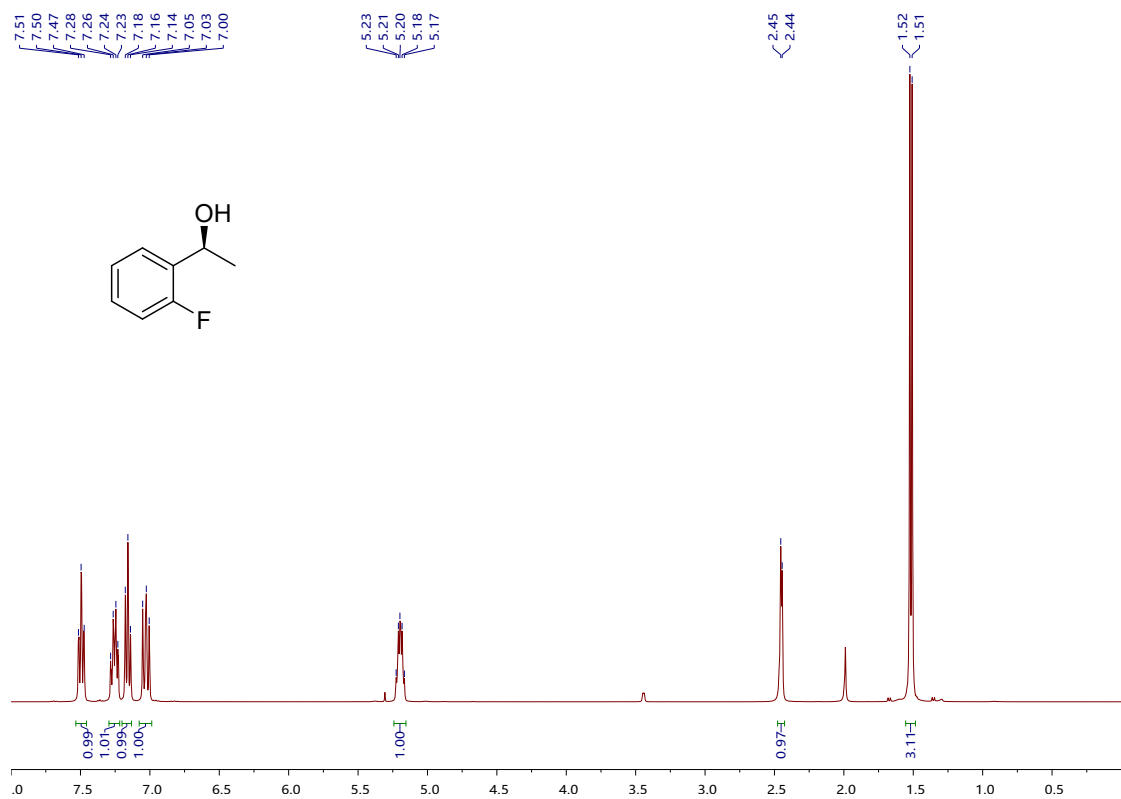










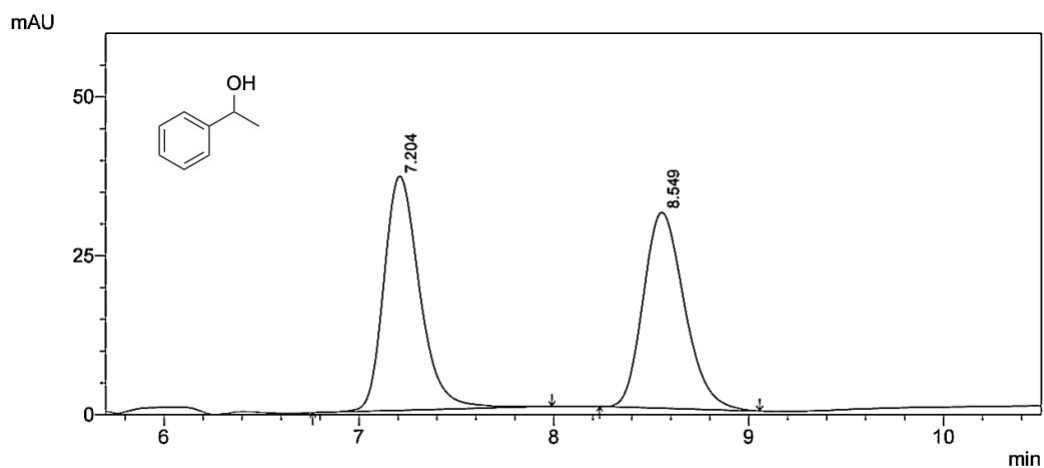


### HPLC and GC traces of products:

To rigorously establish the absolute configuration, the chiral HPLC (High Performance Liquid Chromatography) and GC (gas chromatography) analysis of the obtained chiral alcohol compounds were conducted using authentic standards as reference.

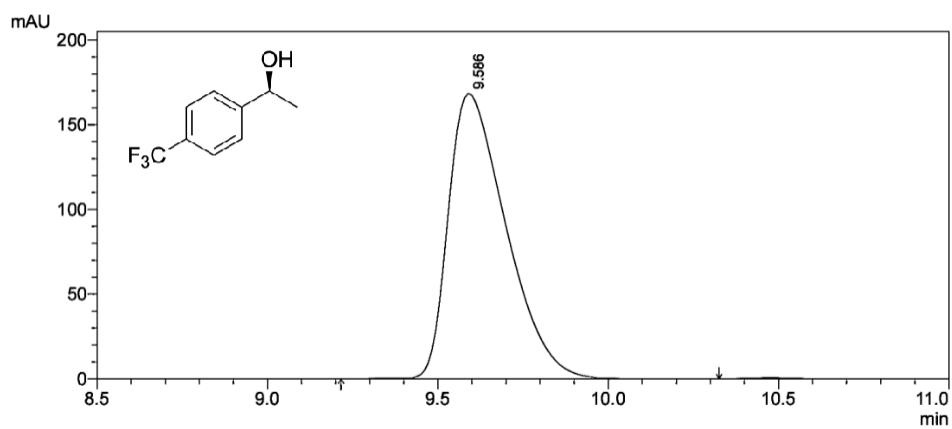
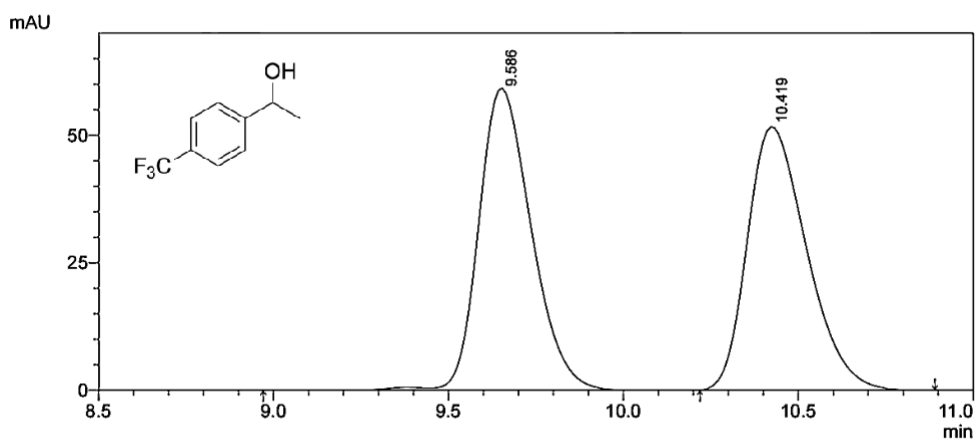
#### 1-Phenylethanol (HPLC)

HPLC system equipped with a UV detector at 254 nm. Column: CHIRALCEL OD-H ( $4.6 \times 250$  mm,  $5 \mu\text{m}$ ), flow rate:  $1 \text{ mL} \cdot \text{min}^{-1}$ , temperature:  $30 \text{ }^\circ\text{C}$ , mobile phase: 2% isopropyl alcohol and 98% hexane,  $t_R = 7.204$  min  $t_S = 8.549$  min.



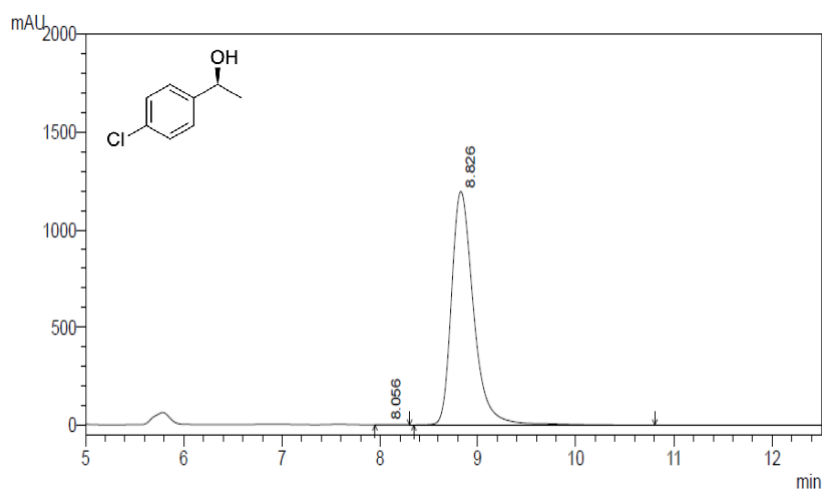
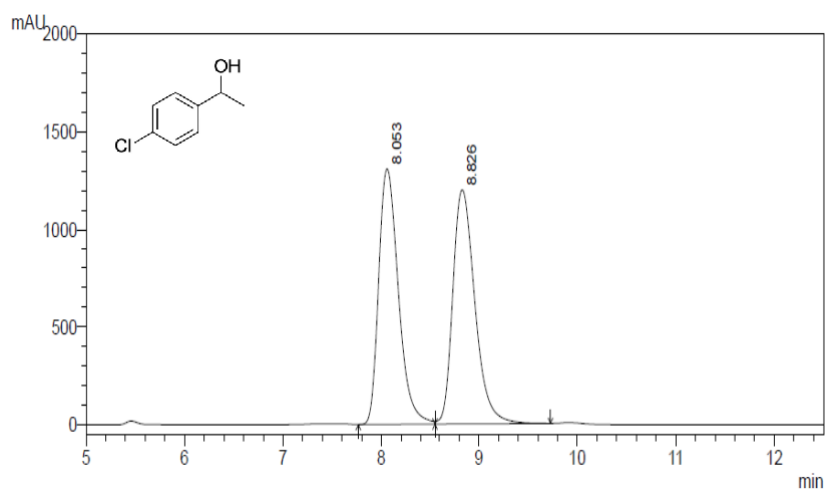
### 1-[4-(Trifluoromethyl)phenyl] ethanol(HPLC)

HPLC system equipped with a UV detector at 254 nm. Column: CHIRALCEL OJ-H (4.6 × 250 mm, 5 μm), flow rate: 1 mL • min<sup>-1</sup>, temperature: 30 °C, mobile phase: 3% isopropyl alcohol and 97% hexane, t<sub>R</sub> = 9.586 min t<sub>S</sub> = 10.419 min.



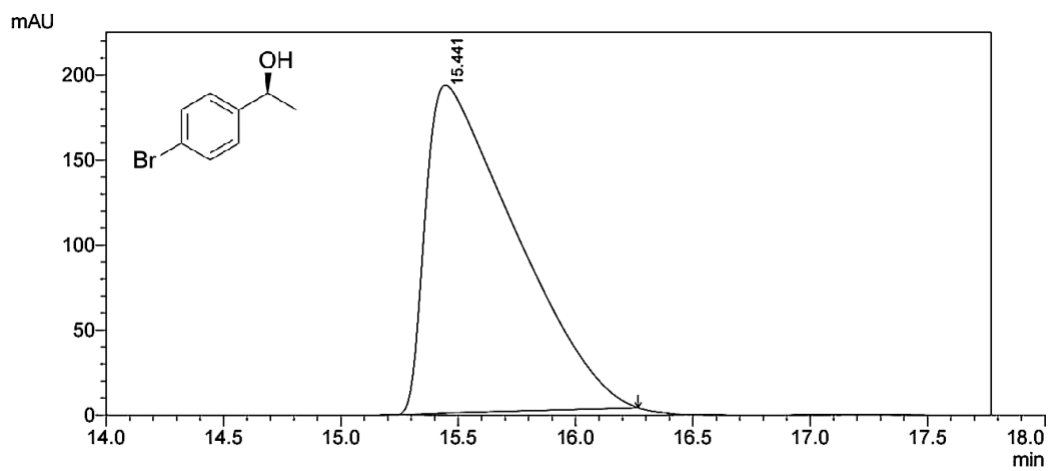
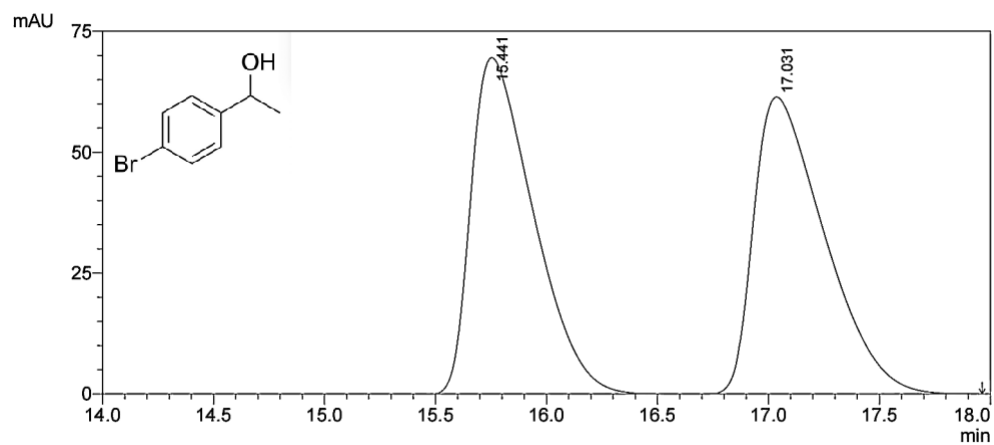
## 1-(4-Chlorophenyl)ethanol (HPLC)

HPLC system equipped with a UV detector at 254 nm. Column: CHIRALCEL OD-H (4.6 × 250 mm, 5 μm), flow rate: 1 mL · min<sup>-1</sup>, temperature: 30 °C, mobile phase: 2% isopropyl alcohol and 98% hexane,  $t_R = 8.053$  min  $t_S = 8.826$  min.



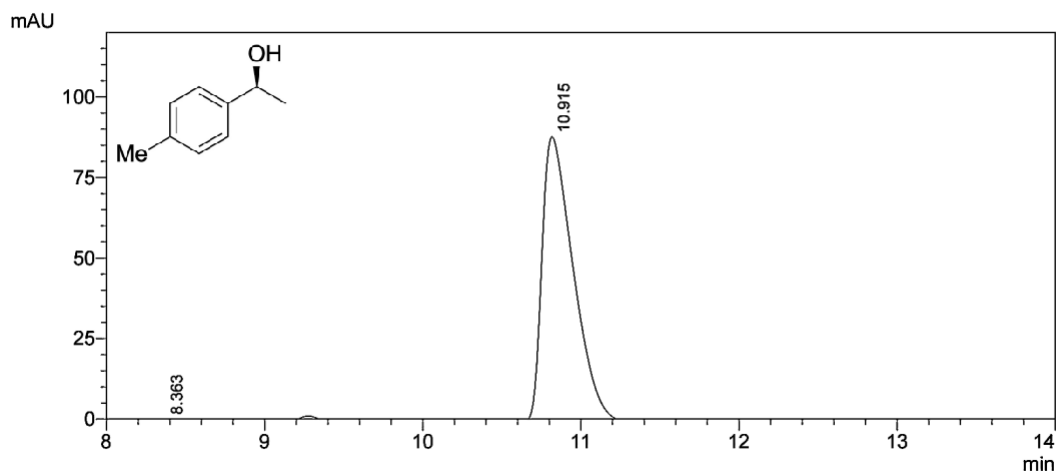
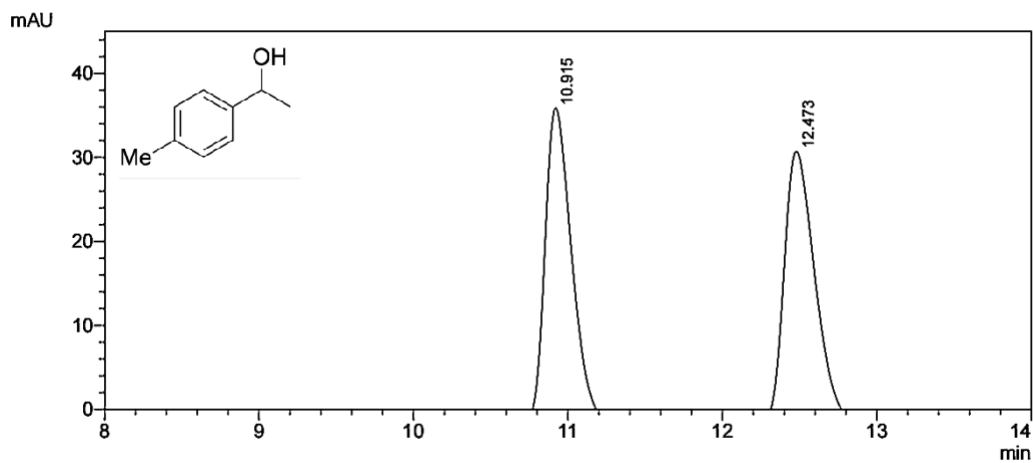
## 1-(4-Bromophenyl)ethanol (HPLC)

HPLC system equipped with a UV detector at 254 nm. Column: CHIRALCEL OD-H (4.6 × 250 mm, 5 μm), flow rate: 1 mL • min<sup>-1</sup>, temperature: 30 °C, mobile phase: 1% isopropyl alcohol and 99% hexane, t<sub>R</sub> = 15.441 min t<sub>S</sub> = 17.031 min.



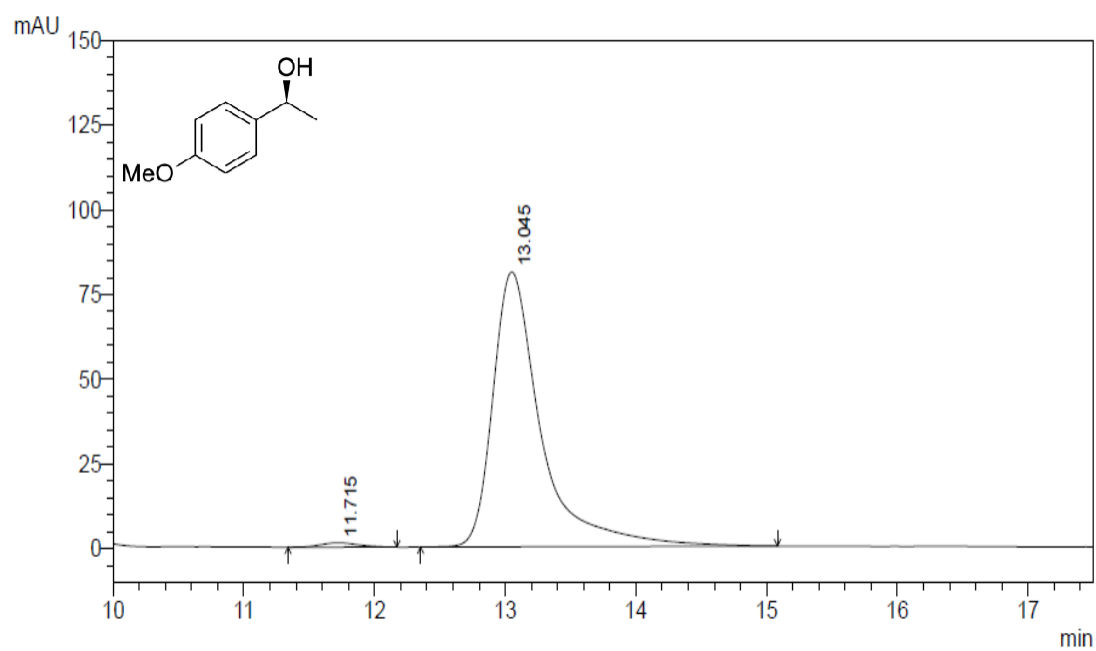
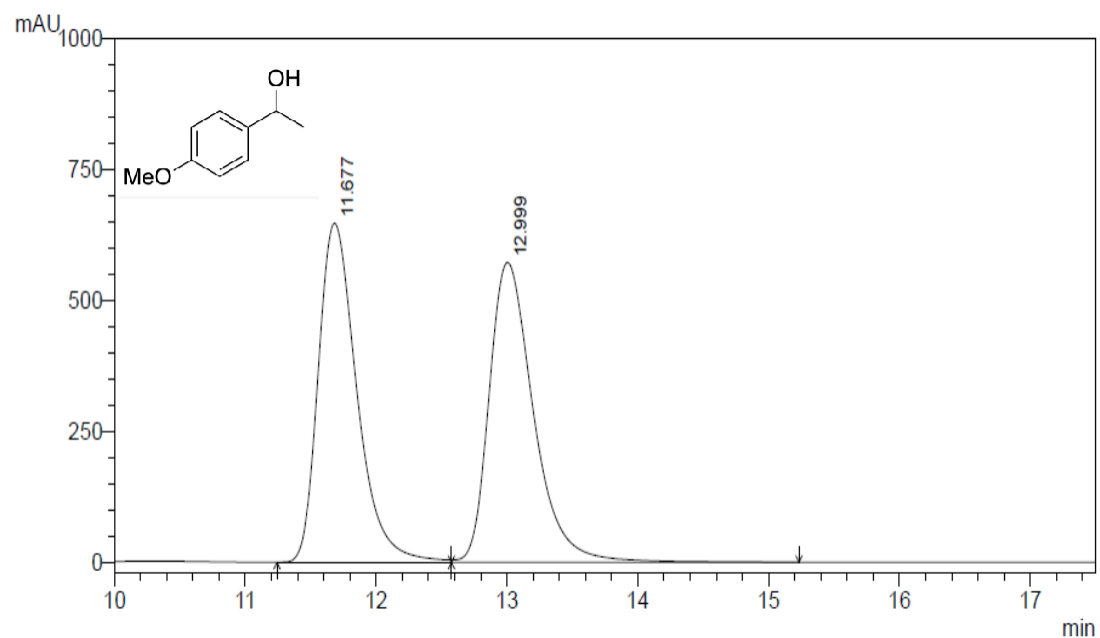
## 1-(4-Methylphenyl)ethanol (HPLC)

HPLC system equipped with a UV detector at 254 nm. Column: CHIRALCEL OJ-H (4.6 × 250 mm, 5 μm), flow rate: 1 mL • min<sup>-1</sup>, temperature: 30 °C, mobile phase: 5% isopropyl alcohol and 95% hexane, t<sub>R</sub> = 10.915 min t<sub>S</sub> = 12.473 min.



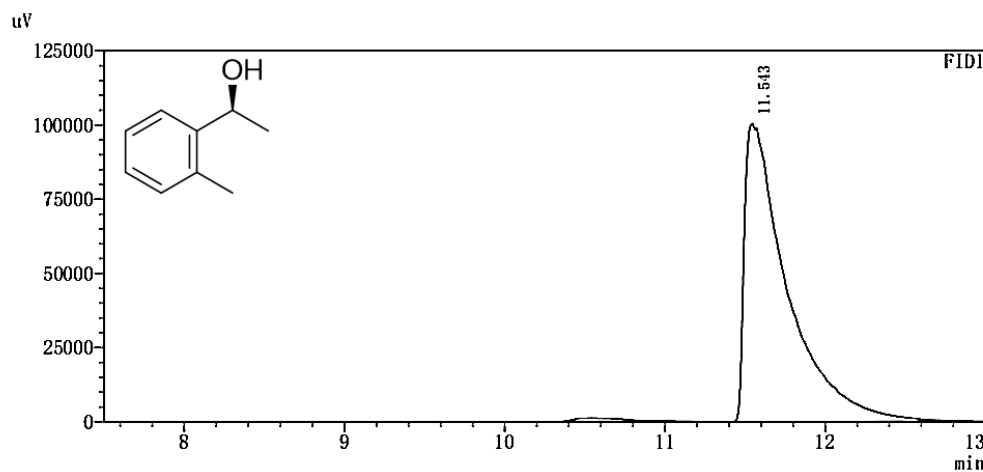
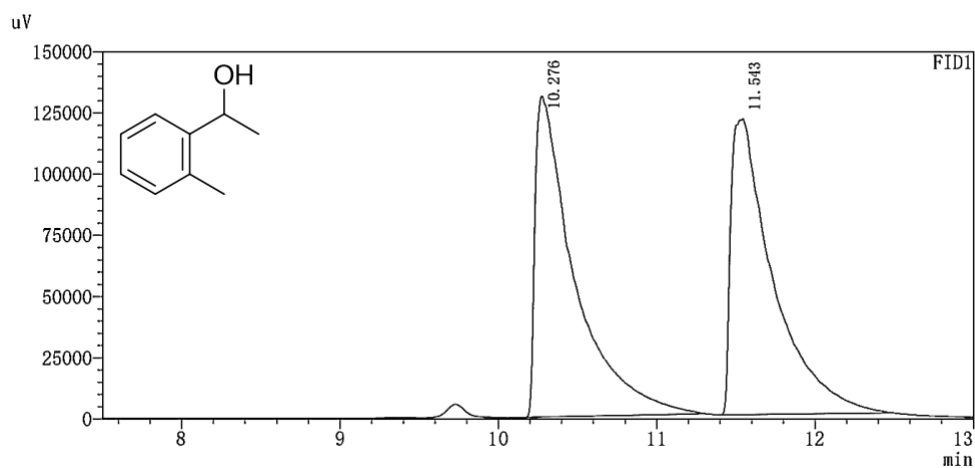
## 1-(4-Methoxyphenyl)ethanol (HPLC)

HPLC system equipped with a UV detector at 254 nm. Column: CHIRALCEL OD-H (4.6 × 250 mm, 5 μm), flow rate: 1 mL · min<sup>-1</sup>, temperature: 30 °C, mobile phase: 3% isopropyl alcohol and 97% hexane,  $t_R = 11.677$  min  $t_S = 13.045$  min.



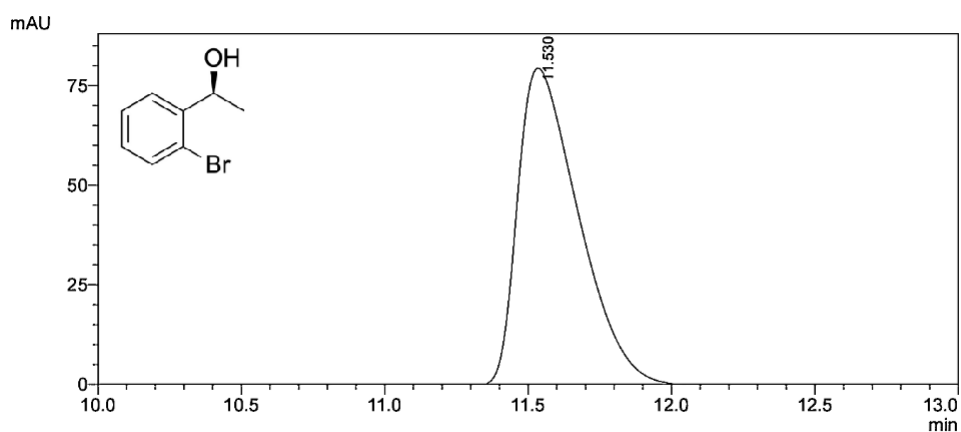
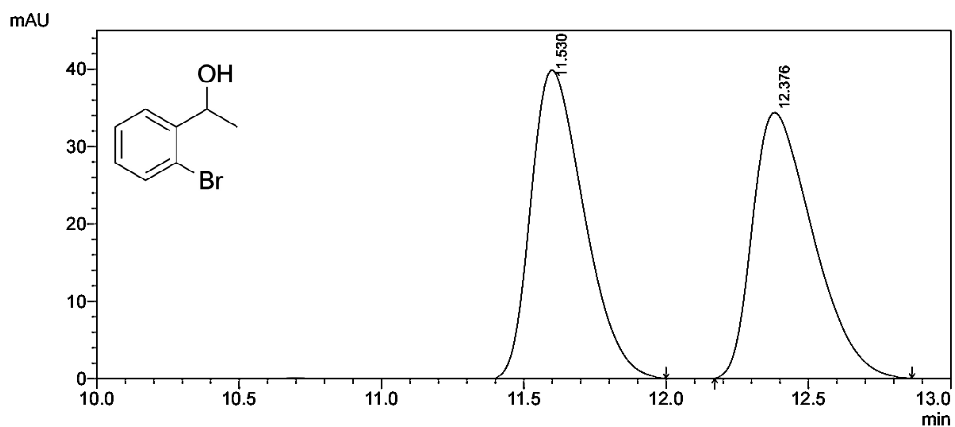
## 1-(2-Methylphenyl)ethanol (GC)

GC conditions: Agilent J&W CP-Chiralsil-DEX CB capillary column (25 m × 0.25 mm × 0.25 μm); carrier gas, N<sub>2</sub> (flow 30 mL/min); initial column temperature 100 °C, hold for 3 min, then, 5 °C/min to 180 °C, hold for 5 min,  $t_R = 10.276$  min  $t_S = 11.543$  min.



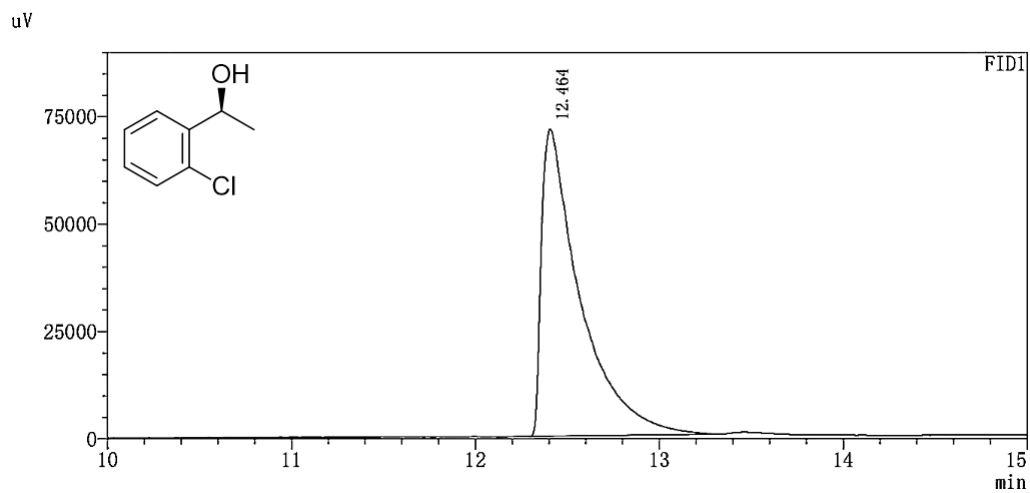
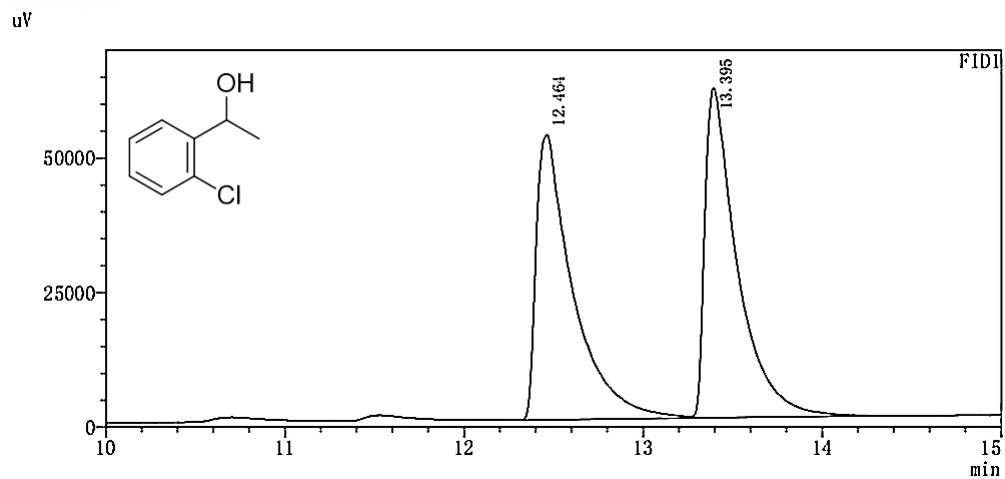
### 1-(2'-Bromophenyl)-1-hydroxyethane (HPLC)

HPLC system equipped with a UV detector at 254 nm. Column: CHIRALCEL OJ-H (4.6 × 250 mm, 5 μm), flow rate: 1 mL · min<sup>-1</sup>, temperature: 30 °C, mobile phase: 3% isopropyl alcohol and 97% hexane,  $t_R = 11.530$  min  $t_S = 12.376$  min.



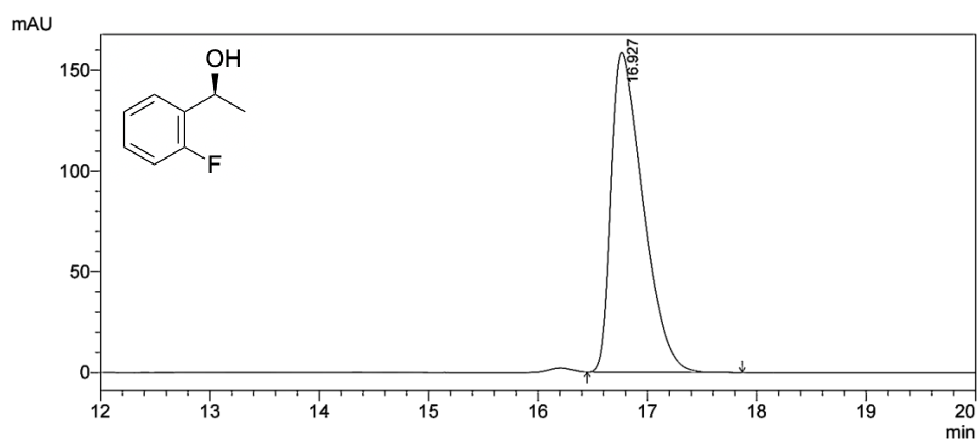
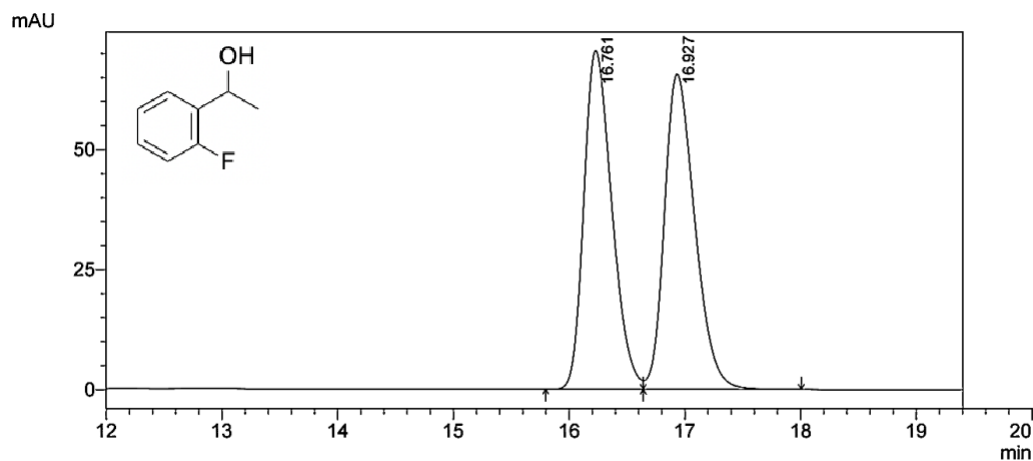
### 1-(2-Chlorophenyl)-1-ethanol (GC)

GC conditions: Agilent J&W CP-Chiralsil-DEX CB capillary column (25 m × 0.25 mm × 0.25 μm); carrier gas, N<sub>2</sub> (flow 30 mL/min); initial column temperature 100 °C, hold for 3 min, then, 5 °C/min to 180 °C, hold for 5 min,  $t_R = 12.464$  min  $t_S = 13.395$  min.



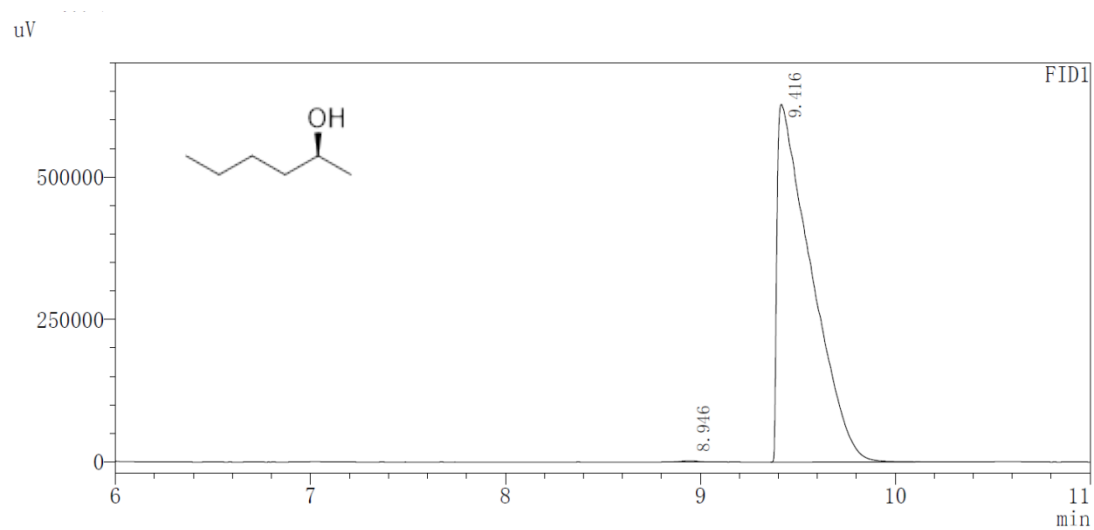
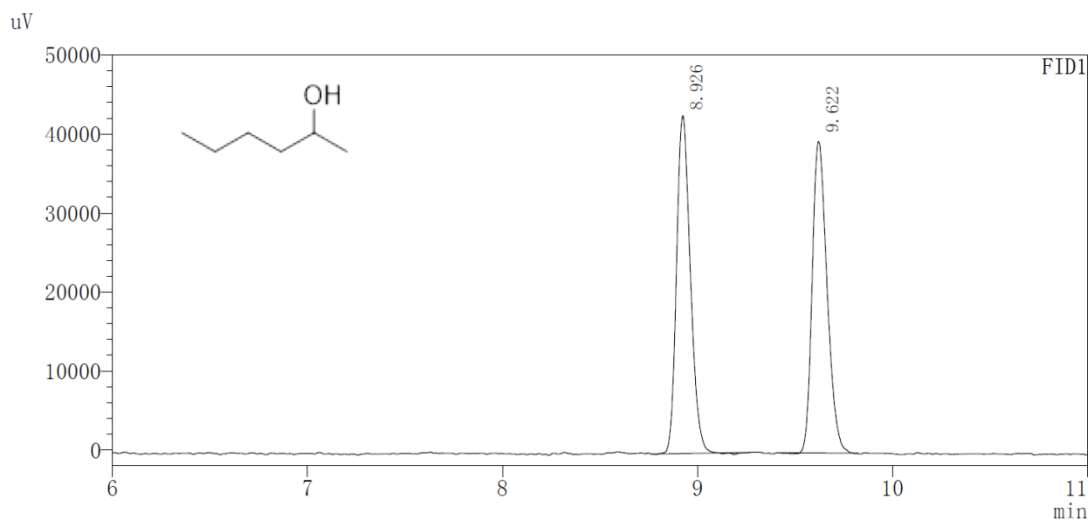
## 1-(2-Fluorophenyl)ethanol (HPLC)

HPLC system equipped with a UV detector at 254 nm. Column: CHIRALCEL OJ-H (4.6 × 250 mm, 5 μm), flow rate: 1 mL · min<sup>-1</sup>, temperature: 30 °C, mobile phase: 1% isopropyl alcohol and 99% hexane,  $t_R = 16.761$  min  $t_S = 16.927$  min.



### (S)-2-Hexanol (GC)

GC conditions: Agilent J&W CP-Chiralsil-DEX CB capillary column (25 m × 0.25 mm × 0.25 μm); carrier gas, N<sub>2</sub> (flow 30 mL/min); initial column temperature 100 °C, hold for 3 min, then, 5 °C/min to 180 °C, hold for 5 min,  $t_R = 8.926$  min  $t_S = 9.622$  min.



### (S)-2-Heptanol (GC)

GC conditions: Agilent J&W CP-Chiralsil-DEX CB capillary column (25 m × 0.25 mm × 0.25 μm); carrier gas, N<sub>2</sub> (flow 30 mL/min); initial column temperature 100 °C, hold for 3 min, then, 5 °C/min to 180 °C, hold for 5 min,  $t_R = 9.883$  min  $t_S = 10.427$  min.

